GEOMORPHIC CONSEQUENCES OF WAVE CLIMATE ALTERATION ALONG CUSPATE COASTLINES

Jennifer Mason Johnson

A thesis submitted to the faculty of the University of North Carolina at Chapel Hill in partial fulfillment of the requirements for the degree of Masters of Science in the Department of Geological Sciences.

Chapel Hill
2013

Approved By:

Laura J. Moore

Tamlin Pavelsky

Antonio Rodriguez

ABSTRACT

JENNIFER MASON JOHNSON: Geomorphic Consequences of Wave Climate Alteration along Cuspate Coastlines
(Under the direction of Dr. Laura J. Moore)

Cuspate coastlines are particularly sensitive to changes in wave climate and represent the best type of coastline for detecting initial responses to changing wave conditions. Previous work indicates that Capes Hatteras and Lookout in North Carolina—which are largely unaffected by shoreline stabilization efforts—have become increasingly asymmetric in shape in response to changes in Atlantic wave climate. Using shoreline change observations, nourishment data, wave climate data and model experiments, we find similar responses to wave climate change along Cape Fear, NC, discernible via temporal and spatial patterns of beach nourishment. Analyses of cuspate features in areas where the change in wave climate has been less pronounced (e.g., Fishing Point, MD & VA) or where local geology likely controls coastline shape (i.e., Cape Canaveral, FL), suggest that coastline shape changes in response to shifting wave climate are currently limited to sandy wave-dominated coastlines where wave climate changes are most pronounced.

TABLE OF CONTENTS

LIST OF TABLES

LIST OF FIGURES

ABBREVIATIONS

CEM – Coastline Evolution Model (Ashton et al., 2001; Ashton & Murray 2006a,b)

DSAS – Digital Shoreline Analysis System (Thieler et al., 2000)

EPR – End-Point Rate

GPS – Global Positioning System

LiDAR – Light Detection and Ranging

LRR – Linear Regression Rate

NASA – National Aeronautics and Space Administration

NOAA – National Oceanic and Atmospheric Administration

SCRD – Shoreline Change Rate Difference

USGS – United States Geological Survey

VCR/LTER – Virginia Coast Reserve Long-Term Ecological Research Project

Chapter 1

Introduction

Coastal environments are highly dynamic, changing dramatically across a range of temporal and spatial scales in response to natural processes and human modifications. Climate change will influence coastal evolution by increasing sea level rise rates (IPCC, 2007), and potentially by increasing the frequency of intense hurricanes (Webster *et al.*, 2005, Knutson *et al.*, 2010). Predicted increases in the rate of sea-level rise over the next century could result in increasing rates of landward translation of barrier islands (e.g., FitzGerald *et al*., 2008; Moore *et al.*, 2010), and changes to ocean wave climate due to changes in hurricane activity, or wave direction, may alter longshore sediment transport gradients and shift erosion hazard areas alongshore (Adams et al., 2011; Moore *et al.*, in review). As coastlines change in response to these forcings, the tendency for humans to exert influence on coastal dynamics is also likely to increase (e.g., McNamara and Keeler, 2013*)*.

Approximately 13% of the world's urban areas, including an estimated 634 million inhabitants, lie in low-elevation coastal zones (McGranahan *et al.*, 2007). Consequently, humans have employed many techniques to mitigate the effects of rising sea level and storms. These techniques, such as shoreline armoring, beach nourishment and artificial dune construction, often have adverse effects that significantly alter sediment fluxes and the natural migration of coastal environments (e.g., Tait and Griggs, 1990; Pilkey *et al.*, 1998; Magliocca *et al*., 2011; Slott *et al.* 2010; Ells and Murray,

2012). Shoreline armoring generally leads to increased narrowing of beaches (Plant and Griggs, 1992) while beach nourishment is expensive and requires repeated applications over extended periods of time (Valverde *et al.*, 1999). An understanding of the coupled processes that alter coastal evolution is becoming increasingly important as our planet continues to change under the influence of natural and human processes.

Background

Recent changes in regional wave climate (the proportion of energy approaching the shore from various angles) have been documented by Komar and Allan (2008). The authors analyzed 30 years of data from 3 buoys and found a trend of increasing summer season significant wave heights, especially for large waves (i.e., hurricane-generated), along a stretch of coast from New Jersey to South Carolina, with the magnitude of change increasing southward. They attribute this shift to increases in hurricane intensity observed by Emanuel (2005). The hurricane-generated waves (heights > 3m) off the coast of Cape May, NJ have increased by an average of 0.011m/yr between the mid-1970s and 2005, while those off Cape Hatteras, and Wilmington, NC and Charleston, SC increased in height by an average of 0.7m and 1.8m respectively over the same time period (Komar &and Allan, 2008). McNamara et al. (2011) found that when summer season significant wave height increases off the coast of North Carolina, the wave climate—defined as the distribution of wave influences from different directions—becomes increasingly asymmetric, with a greater proportion of the influence on alongshore sediment flux coming from waves approaching from the east and northeast.

Sustained changes in the relative influences of waves coming from different directions will ultimately alter the shape of a coastline. Cuspate coastlines, which are characterized by high curvature (e.g., the coast of North Carolina in the U.S.), are particularly sensitive to changes in wave climate (Ashton and Murray, 2006a, 2006b, Slott et al., 2006) and are therefore likely to

respond more quickly than straighter stretches of coast. Model simulations of a cuspate coastline using the Coastline Evolution Model (CEM; Ashton and Murray, 2006a) predict that increased patterns of storminess and associated wave climate alterations could result in cape tip accretion rates up to 11 m/yr and erosion rates up to 4m/yr in the cuspate bays (Slott et al., 2006). Prolonged beach nourishment activities can dramatically change the way a cuspate coastline responds to a shift in wave climate, relative to what would occur without nourishment. Comparing the results of numerical model experiments with and without nourishment (both involving the same wave-climate change scenario) suggests that the shoreline-change effects attributable solely to even an isolated zone of nourishment could exceed the magnitude of change expected from sea-level rise (Slott et al., 2010)—and that these anthropogenic effects can extend surprising distances up- and downdrift from the shoreline stabilization. In addition, Ells and Murray (2012) showed that with hard-structure stabilization, anthropogenic impacts on large-scale coastline change can be greater in magnitude than with nourishment, and exhibit a qualitatively different pattern.

To determine if effects of wave climate change are already discernible, Moore et al. (in review) determined the difference between historic rates and recent rates of shoreline change along stretches of the North Carolina coast (including Cape Hatteras and Cape Lookout). They compared these observations with model predictions for the response of a cuspate coastline to a wave climate specifically altered to reflect the increased summer significant wave-height trend identified by Komar and Allen (2008). Results (Moore et al. in review) suggest that the observed pattern of increasing erosion (accretion) along northern (southern) flanks of both capes is consistent with the model predicted change in coastline shape expected to arise from the wave climate change identified by Komar and Allan (2008).

The two cape features examined by Moore et al. (in review) show a distinct geomorphic signature of wave climate change. Both are located near the zone of maximum summer significant wave-height increase identified by Komar and Allan (2008) and have been relatively

unaltered by human activities. We can expect coastline response to wave climate change to be different or less detectable in areas where the change in wave climate is less pronounced or in areas where human shoreline stabilization affects coastline response. Where human and natural influences are coupled, the resulting system can exhibit complex responses to changes in forcing. For example, McNamara and Werner (2007) and McNamara et al. (2011) demonstrate that complex, emergent behaviors can result from the interactions of economics, human decisions and coastal evolution.

Here, I present an analysis of shoreline change observations, beach nourishment records, wave data and model simulations for three cuspate landforms on the U.S. East Coast (Cape Fear, North Carolina, Fishing Point, Maryland & Virginia and Cape Canaveral, Florida) to determine if the effects of wave climate change - such as those found on largely-unaltered Capes Hatteras and Lookout by Moore et al., (in review) - are discernible in areas where changes in wave climate has been more subtle (e.g. Fishing Point) and where the coast has been modified by humans (e.g. Cape Fear).

Study Areas

I examined three cuspate coastal landforms along the U.S. Mid-Atlantic coast; the highly-altered Cape Fear in North Carolina (Fig. 1a)**,** a northern location including portions of the Delmarva Peninsula near Fishing Point, considered by some to be a 'false cape' (e.g., Leatherman et al., 1982) (Fig. 1b), and the region surrounding Cape Canaveral, Florida (Fig. 1c). Each study area (encompassing the stretch of coast approximately 30km to the north and south of the cape tip) has experienced a unique combination of wave climate change and human alteration as outlined below.

Cape Fear, the southernmost of the three capes that characterize the coast of North Carolina, lies just south of Wilmington, NC (Fig. 1a and 2a). The northern flank of this cape, extending from Kure Beach to Fort Fisher, is considered part of the mainland, but features low-lying sandy

shorelines, similar to a barrier island. The barrier islands along the southern flank of Cape Fear are primarily composed of channel-fill and are more tide-dominated (i.e. punctuated by a greater number of inlets) than counterparts to the north (Riggs et al., 1995). Relative sea level rise (RSLR) rates along the North Carolina coast have been between 3.0 mm/yr and 3.3 mm/yr throughout the twentieth century (Kemp et al., 2009). The coast adjacent to Cape Fear has been nourished repeatedly since the 1930s, particularly along Kure, Carolina, and Wrightsville Beaches (USACE, 1965; USACE, 1998; Valverde et al., 1999) (Fig. 2a). This is in contrast to locations studied by Moore et al. (in review) in part because Cape Hatteras and Cape Lookout lie within their own respective national seashores and are therefore managed by the National Park Service, remaining relatively free from direct human influence (Valverde et al., 1999). Though Cape Fear differs from the other two NC capes in its degree of human manipulation, it exhibits similar morphology and is subject to the same high-angle wave climate and southerly net alongshore transport direction as Capes Hatteras and Lookout (Ashton and Murray, 2006a). The change in wave climate at Cape Fear is also likely to be similar to the change in wave climate at Capes Hatteras and Lookout because they are located in the same region, bracketed by the buoys showing the increase in hurricane-generated wave heights (Komar and Allen, 2008). For this reason, Cape Fear is an ideal location in which to assess the detectability of a geomorphic signature of wave climate change in the presence of human alteration to the coastline.

Approximately 200 kilometers north of Cape Hatteras, Fishing Point lies along the Delmarva Peninsula and includes coastline from southern Maryland and Virginia (Figs. 1b and 2b). Barrier islands in the study area extend ~30 km north and south of Fishing Point and include a portion of Assateague Island National Seashore (ASIS) in the north, and Wallops Island, Assawoman Island, Metompkin Island, Cedar Island and Parramore Island to the south. The latter two islands are located in the Virginia Coastal Reserve's Long Term Ecological Research site (VCR LTER). The islands of this region are mixed-energy barriers associated with average offshore wave heights of 0.86 m, a tidal range of approximately 1.24 m, and a modern RSLR rate of

approximately 4.3 mm/yr (Hayes, 1979). The five barrier islands south of Fishing Point are retreating along their whole lengths, except for Parramore Island which exhibits alternating patterns of erosion and accretion at each end associated with changes in ebb channel location within the surrounding large ebb tidal deltas (Leatherman et al., 1982; Fig. 2b). Direct human influence here is relatively minimal (Valverde et al., 1999), with the exception of Wallops Island, which is home to NASA's Goddard Space Flight Center Wallops Flight Facility (WFF). The shoreline near the WFF has been the site of repeated shoreline stabilization efforts over the last century (NASA, 2010)—currently a seawall is being repaired and extended (WFF, 2011), and an associated nourishment project is scheduled for the near future (WFF, 2010). Because the strength of the hurricane-wave-height trend found by Komar and Allan (2008) decreases to the north , wave climate change along the Delmarva Peninsula has likely been less pronounced than it has along the North Carolina coastline (although shifts in wave-angle distribution could occur for other reasons).

Cape Canaveral (formerly Cape Kennedy) is approximately 660 km south of Cape Fear on the coast of east central Florida and lies on a peninsula, which hosts the Cape Canaveral Air Force Station. In 1950, construction began on an artificial inlet (Port Canaveral) just south of the cape tip, which requires high rates of dredging to counter high rates of alongshore sediment transport (Work and Dean, 1990). The peninsula itself is composed of a series of northeast trending beach ridges that date to ~ 4,000 to 150 B.P. (Rink and Forest, 2005). Approximately 3km north of the tip of Cape Canaveral is an area known as "False Cape," home to the Kennedy Space Center shuttle launch area (Fig. 2c). Komar and Allan (2008) did not extend their analysis southward beyond the Charleston buoy (most directly offshore of Wilmington, NC). However, because the trend of increasing summer season significant wave height increases southward (Komar and Allan, 2008), I can reasonably assume that this region has also experienced an increase in hurricane-generated waves.

I hypothesized that if changes in patterns of shoreline erosion and accretion (and therefore coastline shape) are not apparent in observations of Cape Fear, this will likely be because shoreline stabilization efforts have masked the response of the coastline to an increasingly asymmetric wave climate. I also hypothesized that changes in wave climate may be too subtle to produce a detectable change in patterns of shoreline erosion and accretion in the vicinity of Fishing Point, MD and that changes in wave climate along the eastern Florida coast may have altered the shape of Cape Canaveral over the last several decades.

Methods

Historical Shoreline Change Analysis

To conduct a shoreline change analysis for the north and south flanks of Cape Fear, Fishing Point and Cape Canaveral, I gathered all available digital shoreline shapefiles (Tables 1-3) and used them to quantify and compare shoreline change rates pre- and post- 1975 (which I refer to as historic and recent time periods, respectively). I selected the 1975 breakpoint between historic and recent rate calculations to coincide with the beginning of the time period of wave observations analyzed by Komar & Allan (2008). Available shorelines include 8 historic and 4 recent shorelines for Cape Fear (USGS, 2011; NOAA, 2011, NCDCM, 2011), 6 historic and 8 recent shorelines (for the area surrounding Fishing Point (USGS, 2012; Oster, 2012; ASIS, 2012), and 11 historic shorelines and 11 recent shorelines for Cape Canaveral (USGS, 2012; NOAA, 2012; FF&W, 2012). Though some of these shorelines offer only partial coverage of the study areas, I included all shorelines in shoreline change rate analyses to provide the most

representative measure of shoreline change possible. (A summary of shoreline metadata, including year(s) of survey, source, coverage extent, and original datum appears in Tables 1-3.)

Following methods outlined by Moore et al. (2000), I calculated shorelines change rates for each time period using the Digital Shoreline Analysis System (DSAS) for ArcGIS (Thieler et al., 2000). Prior to calculating shoreline change rates, I projected all shorelines into the State Plane Coordinate System and created an offshore baseline representing a visual average of (i.e., having the same general shape as) all shorelines. Using DSAS, I cast transects at 100 m spacing from the baseline through the shorelines to intersect at roughly perpendicular orientation. The points where transects intersect the shorelines are then used to compute a linear regression rate (LRR) of shoreline change along each transect for each time period (a and b in Figs 2, 3 & 4). Inclusion of shoreline change rates in zones dominated by short timescale processes (i.e. cape tips and inlets) produce high rates of change dominated by inlet/tidal processes rather than the wave-dominated processes of interest in this study. Therefore, I removed transects and did not calculate rates of change for regions of cape and inlet influence as qualitatively identified by zones where the shorelines were no longer roughly parallel to one another and within roughly 2km of cape tips, respectively. Additionally, because a 1975 shoreline was not available for the Cape Fear location, I shifted the breakpoint for Cape Fear to 1970.

For some time periods and stretches of coast only two shorelines were available, making calculations of LRR impossible. In this case, I calculated an end point rate (EPR) (Historic Cape Fear had ~60% LRRs, 40% EPRS; Recent Fishing Point ~95%LRRs, 5%EPRs; Historic & Recent Cape Canaveral ~72% LRRs, 28% EPRs). (See Appendix A for additional information regarding the exact location and extent of LRRs vs. EPRs.) After calculating shoreline change rates, I applied a Gaussian filter (1km for Cape Fear and Cape Canaveral, and 600m for Fishing Point) to each set of rates to aide in identifying large-scale trends. Because transects (and therefore shoreline change rates) within a window equal to the filter length are lost at the end of

each dataset and adjacent to gaps within a data set (e.g. between islands or on either side of an inlet-influenced shoreline), I chose a filter length that was as short as possible to minimize data loss, while also choosing a length long enough to highlight general trends in shoreline change rates across the study area. Because the Fishing Point study area consists of several discrete islands, I applied a shorter filter length across this region than I did the other two study areas.

To determine shifts in patterns of erosion and accretion, I calculated the difference in shoreline change rates (SCRDs) between historic and recent time periods by subtracting the historic rates of shorelines change (R_h) from the recent rates of shoreline change (R_r).

$$\textit{Shoreline Change Rate Difference (SCRD)} = R_r - R_h$$

Thus, positive (negative) SCRD values indicate an increasingly accretional /less erosional (erosional/less accretional) trend since the observed onset of an increasingly asymmetric wave climate.

Beach Nourishment Data

I downloaded data regarding the timing and volume of beach nourishment along both flanks of Cape Fear from the Program for the Study of Developed Shorelines (PSDS, 2012). During the time period 1939 to 2010, approximately 70 percent of the Cape Fear study area was nourished at some point. Data from PSDS include nourishment volumes and the length of coastline along which nourishment sand was distributed for individual communities. I divided the episodes of nourishment into five-year bins to more easily discern general trends in nourishment volume through time (Fig. 3). I then determined the cumulative nourishment sand volume along both flanks of Cape Fear and calculated regression rates for each of three time periods having different rates of sand emplacement.

To discern spatial patterns in nourishment activity I separated the nourishment episodes by community. I then selected a representative community length to calculate a normalized nourishment volume per meter of shoreline per community. I chose the community length by determining the longest alongshore length of a single nourishment episode as given for each community in the PSDS (2012) data (Appendix B). I did not analyze nourishment volumes on the southern flank of Cape Fear because nourishment activities began only after the onset of the observed changes in wave climate.

Wave Climate Change Analysis

Komar and Allan (2008) analyzed data from wave buoys, yet their analysis did not include areas in the vicinity of Fishing Point and Cape Canaveral, presumably because wave buoys are not available there. To analyze both the change in wave height and direction in the vicinity of Fishing Point and Cape Canaveral, I gathered data sets from 41 Wave Information Studies (WIS) stations (22 from FP and 19 from Cape Canaveral). (WIS data can be downloaded from wis.usace.army.mil). Using measured wind speed and directional data, WIS stations provide hindcasts of significant wave height at 3-hour intervals from ~1980 to 1999. Following the analysis of buoy data by Komar and Allan (2008), for each station I calculated a linear regression for both summer season (July-Sept) and hurricane season (June – Nov.) significant wave height. I then separated waves greater than 3m in height, identified as hurricane-generated waves when occurring in the summer months (Komar and Allan, 2008), and determined the rate of wave height increase (Figs. 4 and 5). All trends are significant at the 95% confidence level using the Wilcoxon rank-sum test.

To assess the directional effects of the changes in summer (or hurricane) season significant wave heights on wave climate I examined changes in wave approach angle. I identified a general shoreline trend (28° for Fishing Point and 340° for Cape Canaveral), which I was used to determine the relative wave approach angle. I calculated probability distribution

functions (PDFs; representing the relative influence on alongshore sediment flux from different offshore wave-approach directions) for the overall annual wave climate, the summer months (July – Sept.), the non-summer months (Oct. – June) (Figs. 6 and 7), hurricane season (June – Nov.) and non-hurricane season (Dec. – May). (See Appendix C for analysis from all WIS stations used in this study).

Coastline Evolution Model Simulations

In collaboration with Kenneth Ells at Duke University, we used the Coastline Evolution Model (CEM) (Ashton and Murray, 2006a) to predict how historical nourishment patterns, such as those occurring in the vicinity of Cape Fear, would likely alter shoreline change rates in both the presence and absence of wave climate change. CEM uses a PDF to select a daily offshore wave direction, calculates wave shoaling and refraction over assumed shore-parallel contours until depth-limited breaking occurs, and uses the CERC equation to calculate alongshore transport gradients (Ashton and Murray, 2006a). Perturbations in coastline shape that extend offshore can shadow adjacent coastline segments from incoming wave energy, altering the net rates of alongshore sediment transport.

Gradients in alongshore sediment flux determine shoreline movement. Erosion and accretion are assumed to extend along the equilibrium shoreface profile and the profile shape remains constant. Starting with a simplified straight, sandy coastline and using a PDF based loosely on wave hindcast statistics from WIS station 509, we initially generated a cuspate Carolina-like initial-condition coastline (Slott et al., 2010; Ells and Murray, 2012). For model runs including wave climate change, we initiated a linear

increase in the probability of waves approaching from the east and northeast starting in 1970 (Fig. 8).

To simulate beach nourishment, we chose two locations (along the northern flank of the modeled cuspate feature representing Cape Fear) that approximate the locations of Wrightsville Beach and Carolina Beach relative to the cape tip, because these two communities have historically nourished in large quantities (Fig. 2 and Fig. 9). We initially constrained the extent of nourishment within each 'town' to limited zones alongshore (dark grey bars in Fig. 9). To reproduce the increasing nourishment rates in neighboring communities (e.g. Figure 8 Island and Kure Beach) we expanded these initial zones in model-year 1985 (light grey bars in Fig. 9) allowing the addition of sand sufficient to maintain the 1985 shoreline. CEM calculates the volumes of sand required to stabilize the nourished stretches of coastline each iteration, records that volume, and instantaneously adds that volume of sand to the shoreline (implicitly spread across the shoreface) to maintain the initial shoreline position.

Results

Shoreline Change & Wave Climate

During the historical time period (pre-1970), shoreline change rates for Cape Fear are largely erosional (Fig. 10a). The southern flank has a fairly uniform erosion rate of approximately -0.5 to -1.5 m/yr and though erosion is also widespread on the northern flank, most locations are only slightly erosional (0 to -0.5 m/yr). The few erosion hotspots on the northern flank appear to be associated with historical inlet migration. In contrast, recent rates of shoreline change along the southern flank are close to zero or

accretional, and in some areas rates are greater than 1.5 m/yr (Fig. 10b). The northern flank is also accretional in the recent time period, but a localized zone of high erosion rates occurs south of the Masonboro Inlet Jetty. The shoreline change rate difference (SCRD) indicates that much of the coastline to the north and to the south of Cape Fear has become more accretional since 1970 (Fig. 10c). The recent erosion hotspot on the northern flank just south of Masonboro Inlet appears as an isolated location of highly negative SCRD values, indicating that this erosional trend has developed since 1970. Whereas a more accretional southern flank is consistent with an increasingly asymmetric cape (Moore *et al.*, in review; Slott *et al.,* 2006), the recent accretional trend on the northern flank appears inconsistent with the hypothesized adjustment to a changing wave climate (in the absence of shoreline stabilization).

Farther to the north in the area surrounding Fishing Point, a different pattern of shoreline change emerges (Fig. 11). For the historic time period, the northern flank can be divided into a southern zone of moderate accretion (up to >2.5m/yr) a mid-zone of moderate erosion (up to -1.5 m/yr) and a northern zone of little change (0.5 to -0.5 m/yr) (Fig.11a). Prior to 1975, the area south of Fishing Point was highly erosional (-1.9 to -5m/yr) except for Parramore Island, which was moderately accretional (1.5 to 2.5 m/yr). Since 1975, the entire study area, except for a few short stretches (all less than 1.5 km in length), has been erosional, with the greatest rates of erosion (up to -12.5 m/yr) occurring at the southern end of the south flank near Parramore Island (Fig. 11b). This large increase in erosion rate across the study area is highlighted by negative SCRD values along both the northern and southern flanks (Fig. 11c). A prominent and well-documented exception to this is Wallops Island, where the historically high rate of more

than -2.5m/yr has been reduced to values near zero (-0.5 – 0.5 m/yr) in the recent past as a result of shoreline stabilization efforts designed to protect the NASA Wallops Flight Facility (NASA, 2010). Because the barrier islands along the southern portion of this study area are limited in spatial extent and because inlets have heavily influenced much of the southern portion of the study area over time, there are significant data gaps along the southern flank. As a result, rates are limited in spatial coverage and may not necessarily be representative of overall coastal change in the region.

In the historic time period (prior to 1975), shoreline change rates for Cape Canaveral are generally low (between 1.5 and -0.5 m/yr) except near the cape tip itself (Fig.12a). High rates of accretion near the cape tip on the southern flank gradually decrease southward to near zero (-0.5 m/yr), whereas the high erosion rates near the cape tip on the northern flank (-1.5 to -2.5 m/yr) rapidly decrease northward becoming near zero (0 to -0.5m/yr) and then moderately accretional (0.5 to 2.5 m/yr). (Note: in the northernmost extent of the study area, only two shorelines were available for each time period (1875 and 1924 and 1999 and 2004) and therefore shoreline change rates along this stretch are EPRs rather than LRRs.) In the period since 1970, though shoreline change rates are more variable in the alongshore direction, the north part of the north flank remains largely accretional, with a localized zone of enhanced erosion (-2.5 to -1.5 m/yr) north of False Cape. Immediately south of False Cape, rates are slightly accretional then become slightly erosional (~1.5 m/yr to -2.5 m/yr). Patterns of shoreline change along the southern flank of Cape Canaveral are similar to the historic patterns - rates are highly accretional just south of the cape and transition to roughly zero (±0.5 m/yr) southward. However, immediately north of the cape tip SCRDs indicate the area is

increasingly less erosional, while the area just to the north of the enhanced accretion (directly south of False Cape) is much more erosional (-1.5 m/yr to less than -2.5 m/yr) (Fig. 12c). Another zone of slightly enhanced accretion occurs along False Cape itself whereas a zone of increasing rates of erosion (-0.5 m/yr to -2.5 m/yr) occurs immediately to the north. These observations are in agreement with the analyses of Absalonsen and Dean (2010).

Wave Climate

My wave analysis for Fishing Point is consistent with the range of values reported to the north and south by Komar and Allan (2008) and suggests that both increases in summer season (July – Sept.) and hurricane generated (summer waves over 3 m high) wave height within the vicinity of Fishing Point (WIS Stations 163, 165-178, 180-188) were small (between .0015 and 002 m/yr) (Fig. 4). My analysis for Cape Canaveral (WIS Stations 416-418, 430-440, 518-521) suggests that there was an increase of 0.009 m/yr in summer season significant wave height, and an order of magnitude greater average increase of 0.05 m/yr in hurricane-generated wave height (Fig. 5). When I extended the analysis of stations in the vicinity of Cape Canaveral to include the entire hurricane season (June – Nov.), results were similar – indicating an average increase of 0.008 m/yr in overall hurricane season waves, and an average increase of 0.05 m/yr in hurricane-generated waves.

I examined PDFs representing the relative influences on alonghshore sediment flux from different offshore wave approach angles for the Fishing Point and Cape Canaveral wave climate data (Figs. 6 and 7) to assess the effect of increases in hurricane-generated-wave height on relative influence of waves on alongshore transport. The

analysis reveals an annually bimodal wave climate at Fishing Point, with a greater contribution from waves approaching from the left (northeasterly) (Fig. 6a). During non-summer months, the wave climate is similar to the annual wave climate (Fig. 6b). During the summer months the wave climate appears more strongly bimodal in comparison to the annual wave climate with more waves approaching from high angles and the right (south) (Fig. 6c). Hurricane-generated waves (those > 3m) approach from predominantly high angles, with a greater proportion from the east and northeast (left) than the south (right) (Fig. 6d). Near Cape Canaveral, the wave climate appears low-angle and slightly asymmetric, with a greater influence of waves coming from the left (north/northeast) relative to the general orientation of the shoreline (Fig. 7a). The PDF of wave direction for non-summer months is similar to the annual analysis, displaying only a small change in the proportion of waves approaching from the left at high-angles (Fig. 7b). Conversely, the PDF of wave direction for summer months suggests a slight increase in high-angle waves from the left (north/northeast) (Fig. 7c) while the hurricane-generated waves approach shore from predominantly low-angles with a slight asymmetry to the left (north/northeast) (Fig. 7d).

Nourishment Observations and Modeling

Examining the binned beach nourishment data, I identified three distinct trends (Fig. 3). From ~1935 to 1960, the rate of nourishment was low (32,000 m^3/yr) because relatively few nourishment episodes took place during this time period. After 1960, the rate of beach nourishment in the vicinity of Cape Fear increased by an order of magnitude (to 415,000 m^3/yr) and nearly doubled after 1980 (to 690,000 m^3/yr). Along Wrightsville Beach, nourishment has taken place since the 1930s, and along Carolina

Beach it has taken place since the 1950s, with major episodes of nourishment continuing to present day. The spatial distribution of nourishment through time indicates that nourishment along Wrightsville Beach and Carolina Beach account for over 70% of the total volume of sand emplaced along the northern flank of the cape (34% and 37%, respectively). Because it has the longest history of human alteration of the three study areas, we focused model simulations on the northern flank of Cape Fear to test my hypothesis that the absence of a pattern of shoreline change rates consistent with Moore et al. (in review) suggests that beach nourishment is compensating for, and therefore masking, the effects of wave climate change along Cape Fear.

For model simulations with constant wave climate, the cumulative beach nourishment trend is roughly linear (dashed black line, Fig. 13). This implies a consistent rate of shoreline retreat through time. In this case, the amount of nourishment required each year to stabilize the shoreline remains steady, resulting in a linear trend of cumulative nourishment. However, in model simulations in which the asymmetry of the wave climate is increased (Fig. 8), the rate that nourishment sand needs to be added to maintain shoreline position increases (dotted black lines, Fig. 13). This increase in nourishment rates occurs shortly after the initiation of wave climate change in the model (1970), in response to the tendency for the north flank erosion rates to increase under the increasingly asymmetric wave climate. The black dotted line with open circles (Fig. 10) shows the cumulative nourishment in the model when expansion of the two nourishment zones in 1985 is included.

The solid black line in Fig. 10 shows the observed cumulative nourishment for both towns combined. Little historical nourishment activity occurred from 1940-1960

compared to model results (Fig. 13, black solid line and black dashed line). Around 1965 there is a large increase in observed cumulative nourishment volumes and the gap between observations and model simulations is dramatically reduced. Starting around 1985, the slopes of the cumulative curves representing observations and model results including wave climate change (solid black and circled lines, respectively) are approximately the same, showing that nourishment rates in the model approximately equal those observed during this time period. However, when wave climate change is not included in the model, nourishment rates during this period in the model (slope of dashed black line) are lower than those observed (slope of solid black line).

For simulations in which nourishment occurs within zones representing two towns, modeled nourishment volumes for Town 1 (representing Wrightsville Beach, Fig. 13) – with and without wave climate change (dotted and dashed blue lines, respectively) – are initially (1940 - ~1980) larger than observed volumes (solid blue line). Beginning around 1980 there is a large jump in the observed nourishment volumes and the trends switch such that observed nourishment becomes greater than modeled volumes. In the case of Town 2 (which approximates Carolina Beach, Fig. 13, green lines) modeled nourishment volume is generally higher than observed volumes, except after 1980 in the simulation without wave climate change. Thus, it is the combination of Town 1 simulations slightly under-predicting nourishment and Town 2 simulations slightly over-predicting nourishment that form the cumulative pattern that mirrors the observations of total nourishment volumes along the northern flank of Cape Fear.

Discussion

Moore et al. (in review) have examined two prominent cape features and found significant changes in coastline evolution that are consistent with observed changes in Atlantic Ocean wave climate along the eastern coast of the U.S. Here I have extended that analysis to assess the prevalence of a signature of wave climate change in the evolution of cuspate coastlines in this region under different conditions.

Limitations

The extent and accuracy of the shoreline change analysis is limited by the number of shorelines available. Increasing the number of shorelines lends increased accuracy to analysis (Dolan *et al*., 1991), but not all shorelines extend along the entire study area. While use of LRRs to compute shoreline change is widely accepted, it can be subject to the influence of outliers. Assumptions of a linear trend in shoreline change may not reflect trend reversals or capture cyclical changes in shoreline position (Dolan *et al.*, 1991). However, increasing the length of records to include as many shorelines as possible over the longest time span available reduces these biases (Dolan *et al.*, 1991)

Moore et al. (in review) defined their breakpoint between pre-wave climate change and wave climate change at 1975 because the observations of wave height began in 1975 (Komar and Allen, 2008). Because a 1975 shoreline is not available for Cape Fear, I instead used a breakpoint of 1970 for this study area. If the change in wave climate began before 1975, the use of an earlier breakpoint would increase the contrast between the two time periods and therefore enhance the signature of geomorphic response. If the change in wave climate began closer to 1975, then my inclusion of 1970 in recent shoreline change calculations reduces the difference between the historic and recent time periods, likely decreasing the strength of any geomorphic signature.

However, across such temporal-spatial scales (of years to decades and tens of kilometers) a breakpoint in 1970 instead of 1975 should have negligible impact on my results.

The WIS station (509), used as a guide for choosing the wave climate parameters generating the Carolina-like coast used for model simulations, is located at a position where water depth is considerably deeper than the base of the shoreface. After daily wave angles are selected from the PDFs generated from WIS data, CEM refracts these waves across shore-parallel bathymetric contours, so that wave data from the base of the shoreface would be more appropriate. However, locations that close to the shoreline have other significant drawbacks; wave-shadowing effects prevent any such location from receiving a distribution of waves that is representative of the wave climate affecting the coastline more broadly. Thus, we use WIS station 509 as a rough basis for our wave climates, despite the shortcomings. Since our goal was to use model simulations to explore the main aspects of a large-scale cuspate coastline response to repeated nourishment with and without wave climate change, the potential inaccuracies introduced by the assumption of shore-parallel contours is likely inconsequential to the main results of our analysis.

Nourishment data gathered from PSDS (2012) was grouped according to communities and into 5-year bins, reducing some of the temporal resolution of the data. To represent nourishment in model simulations, I generalized the extent of nourishment by selecting two zones within which nourishment would take place. This simplification still encompasses the regions that account for over 70% of the volume of sand emplaced on the northern flank of Cape Fear.

Moore *et al.* (in review) found that Cape Hatteras and Cape Lookout have become increasingly asymmetric since 1975 in response to an increasingly erosional (accretional) pattern of shoreline change on the northern (southern) flanks of each cape. To link their observations to a change in wave climate, Moore *et al.* (in review) used CEM to confirm that the increasingly asymmetric shape of these cape features could result from an increasingly asymmetric high-angle wave climate reflective of the Komar and Allan (2008) observations. In contrast to Capes Hatteras and Lookout, the SCRD values for Cape Fear are generally accretional on both flanks (Fig.14). While an increasingly accretional southern flank is consistent with an increasingly asymmetric cape, the more accretional signal along the northern flank (with the exception of the more erosional area south of Masonboro Inlet jetty) appears initially inconsistent with the findings of Moore *et al.* (in review).

CEM simulations for the evolution of a nourished, cuspate coastline match observations of shoreline change and beach nourishment trends best when a change in wave climate (consistent with observations; Komar and Allan, 2008) is included (Fig. 13). The simulation results provide strong support for my hypothesis that beach nourishment activities have masked an erosional signal that would otherwise have been visible in recent shoreline change observations along the northern flank of Cape Fear. To stabilize the shoreline, simulations without wave climate change require a steady rate of nourishment to prevent local erosion, which is inconsistent with observations (Fig. 13). Considering overall trends for the region, including an increasingly asymmetric wave climate results in nourishment rates that increase monotonically, consistent with

observations of cumulative beach nourishment volume. This implies that increasing amounts of sand are needed per nourishment episode in an effort to stabilize a stretch of coastline that is increasingly out of equilibrium with changing conditions.

From 1940-1960 (an era without a record of wave climate change) in all simulations, observed nourishment volumes are lower than the modeled volumes needed to maintain a stable shoreline (Fig. 13) which suggests the coast was eroding during that time and that nourishment was not undertaken at a rate sufficient to counter landward shoreline motion. This could be due in part to a smaller coastal population and lack of concern over erosion, or to limited technology available to extract and emplace sand resources at a rate sufficient to counter erosion. From 1960 to ~1985 observed rates of nourishment dramatically increase until the cumulative volume approaches model-generated volumes. This may represent a shift in population, decision-making and/or availability of technology, which led to emplacement of sand via nourishment at a rate sufficient to make up for shoreline erosion in the previous decades. After approximately 1985, in the period where the full spatial extent of nourishment was allowed in the model to be consistent with observed patterns, observed and model-generated nourishment volumes are closely aligned both in magnitude and trend (Fig. 13).

Although shoreline change observations alone do not reflect the geomorphic signature of an increasingly asymmetric wave climate, modeled and natural increases in nourishment volumes through time strongly suggest that the coast was becoming increasingly erosional. With the exception of one location on the north flank of Cape Fear where nourishment has not taken place (i.e. south of Masonboro Inlet) nourishment artificially stabilized the shoreline (reflected in shoreline change patterns) thereby

compensating for coastline changes that would have otherwise occurred. In this case, coastline response to changing wave climate appears to be discernible via changes in the volume of sand emplaced in stabilization efforts.

Though the increase in summer season significant wave height has been smaller in the vicinity of Fishing Point than elsewhere, based on my analysis of WIS data, an increase in hurricane-generated waves would likely result in a slight increase in the influence of waves coming from the east and northeast (Fig. 6d). If this shift were sufficient to alter patterns of erosion and accretion I would expect it to result in a pattern of increasing erosion/less accretion on the northern flank and decreased rates of erosion/more accretion on the southern flank proximate to the cape, in a pattern similar to that observed for the Carolina capes. This is consistent with the pattern of SCRD values on the northern flank and it is also consistent with increasing rates of southward migration of Fishing Point in recent decades. Although the high rates of shoreline change, locally occurring on Parramore Island in the southern portion of the study area, are inconsistent with the pattern of shoreline change we might expect in response to changing wave climate, this stretch of coast is heavily influenced by inlets and rotational island dynamics, the effects of which would likely overwhelm the subtlety of the long-term signal of wave climate change that I have sought to detect here. In addition, Parramore Island is far enough downdrift of the cape that it could be experiencing increased erosion rates as the erosional effects of the wave-shadow zone migrate and propagate downdrift. Given the more subtle nature of wave climate change in this area, it is possible that factors other than wave climate change are resulting in enhanced erosion rates along this stretch of coast in recent decades. For example, Fishing Point is located in a zone of

accelerating sea level rise, related to weakening of ocean circulation patterns in the Atlantic (Sallenger *et al.*, 2012, Ezer *et al.*, 2013) and because this is a region of low-lying islands, negative feedbacks related to overwash frequency and dune-grass species composition may be contributing to widespread shoreline retreat (Wolner *et al., 2013*).

The changes in wave climate around the Cape Canaveral region differ from those observed near Cape Fear and Fishing Point. Directional wave analysis shows that the wave climate (whether the overall, summer months, or hurricane-generated climates) is dominated by low-angle waves, using the regional coastline orientation as a reference. However, consistent with analyses by Absalonsen and Dean (2010), my shoreline change analysis does not reveal shoreline retreat at the False Cape protrusion. In fact, the False Cape shoreline position persists, and may even be advancing seaward, despite the low-angle wave climate. Perhaps more interesting, is the occurrence of Cape Canaveral in the presence of a low-angle wave climate. This initially appears contrary to findings by Ashton et al. (2001) whose work suggests that cape features on sandy coastlines may originate from a high-angle wave climate. Two hypotheses are offered for this apparent discrepancy: (1) it is possible that Cape Canaveral and the False Cape persist in their current configuration because of an underlying geologic control, such as the presence of the Anastasia Formation, which has been thought to impede 'natural' barrier island formation farther south (Finkl *et al*., 2008; Lovejoy, 1983), or alternatively (2) the effects of refraction of the assailing wave field by cape-associated shoals may alter the pattern of longshore sediment transport (LST), setting up LST gradients conducive to a pattern of perturbation growth (Kline et al., in review). Both of these hypotheses offer reasons for shoreline change rates, and SCRD values, that appear contrary to what might be expected

under an increasingly low-angle wave climate. However, further exploration of this possibility is beyond the scope of this manuscript.

Overall, my analysis suggests that coastline response to wave climate change, as well as the detectability of coastline response, is dependent on numerous factors including human intervention, geology, and possibly changes to oceanic circulation. In some regions (e.g. Cape Fear, NC) coastline response to wave climate change may not be observable directly from shoreline change rates, but might instead be evident in records of human alterations to the shoreline. Cape Canaveral and Fishing Point appear to be subject to changes in wave climate, but local factors (i.e. less-pronounced changes in wave climate, underlying geology, or the presence of complex nearshore bathymetry) may suppress coastline response to these changes.

If changes in mid-Atlantic wave climate continue, new and continued shifts in alongshore patterns of erosion and accretion may occur and extended beyond cuspate features, resulting in regional changes in the locations of erosional 'hot spots.' This would likely alter the spatial distribution of beach nourishment activities, potentially leading to new areas of nourishment and increasing competition for available nourishment sand (e.g. McNamara *et al.*, 2011). If predicted increases in hurricane intensity are realized in the future, wave climate change and the consequent coupling of the human and coastline systems may be enhanced along sandy coastlines that are not pinned in position by other factors.

Conclusion

Using a combination of shoreline change analysis, nourishment observations, wave analysis and model simulations I have established a pattern of human intervention that reflects a change in the wave climate near Cape Fear, NC. Other regions (i.e. Fishing Point, Cape Canaveral) may be experiencing changes in wave climate, but due to the numerous complicated processes that shape our coastlines, any specific change related to wave climate cannot currently be detected. Human-induced climate change can lead to further alterations to wave climate which could result in more dramatic shifts in alongshore transport gradients. Human response to these changes can have significant impacts on the shape of the coastline.

Tables and Figures

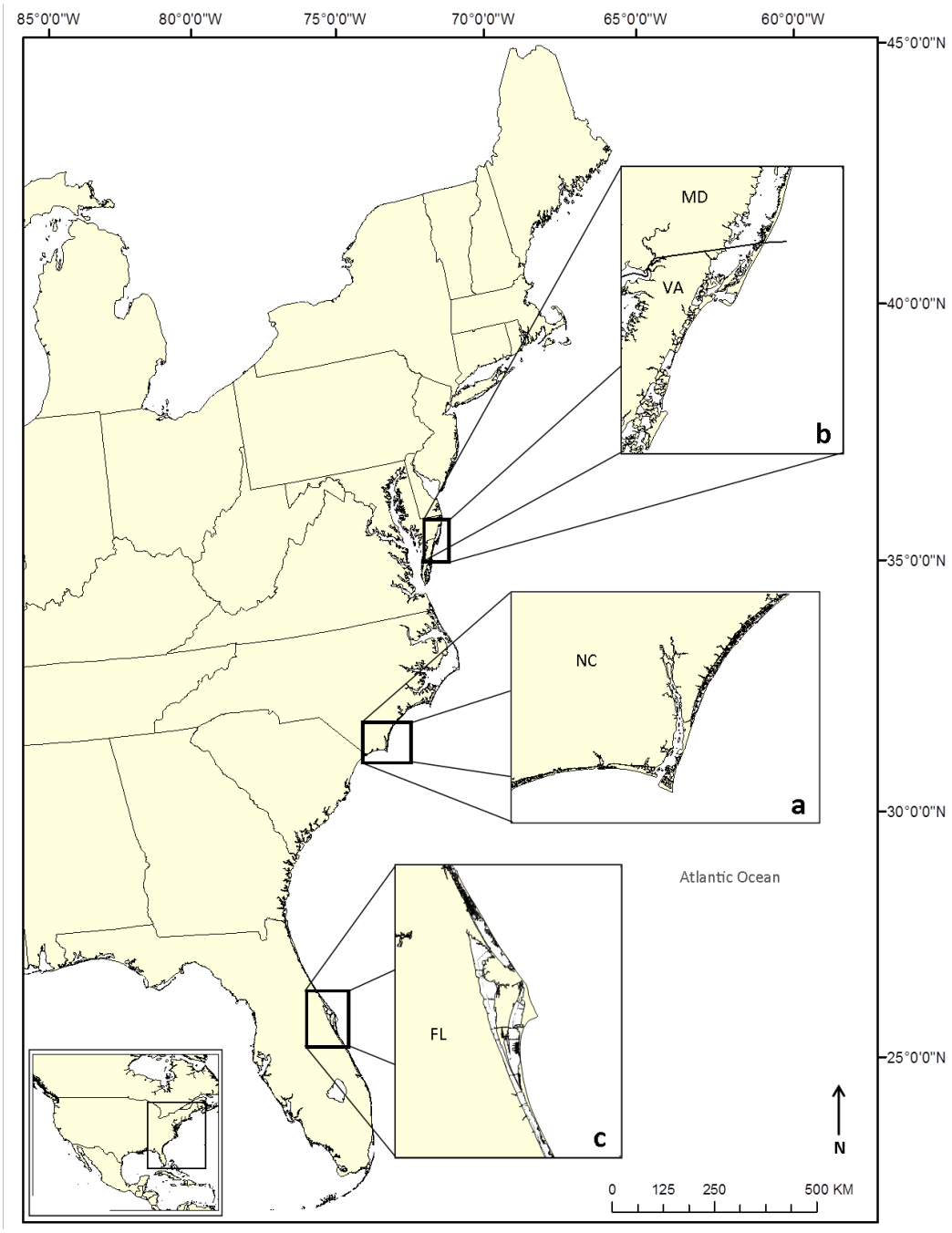

Figure 1. Location of cuspate coastline study areas along the eastern USA are (a) Cape Fear, North Carolina. (b) Fishing Point, VA & MD. and (c) Cape Canaveral, FL.

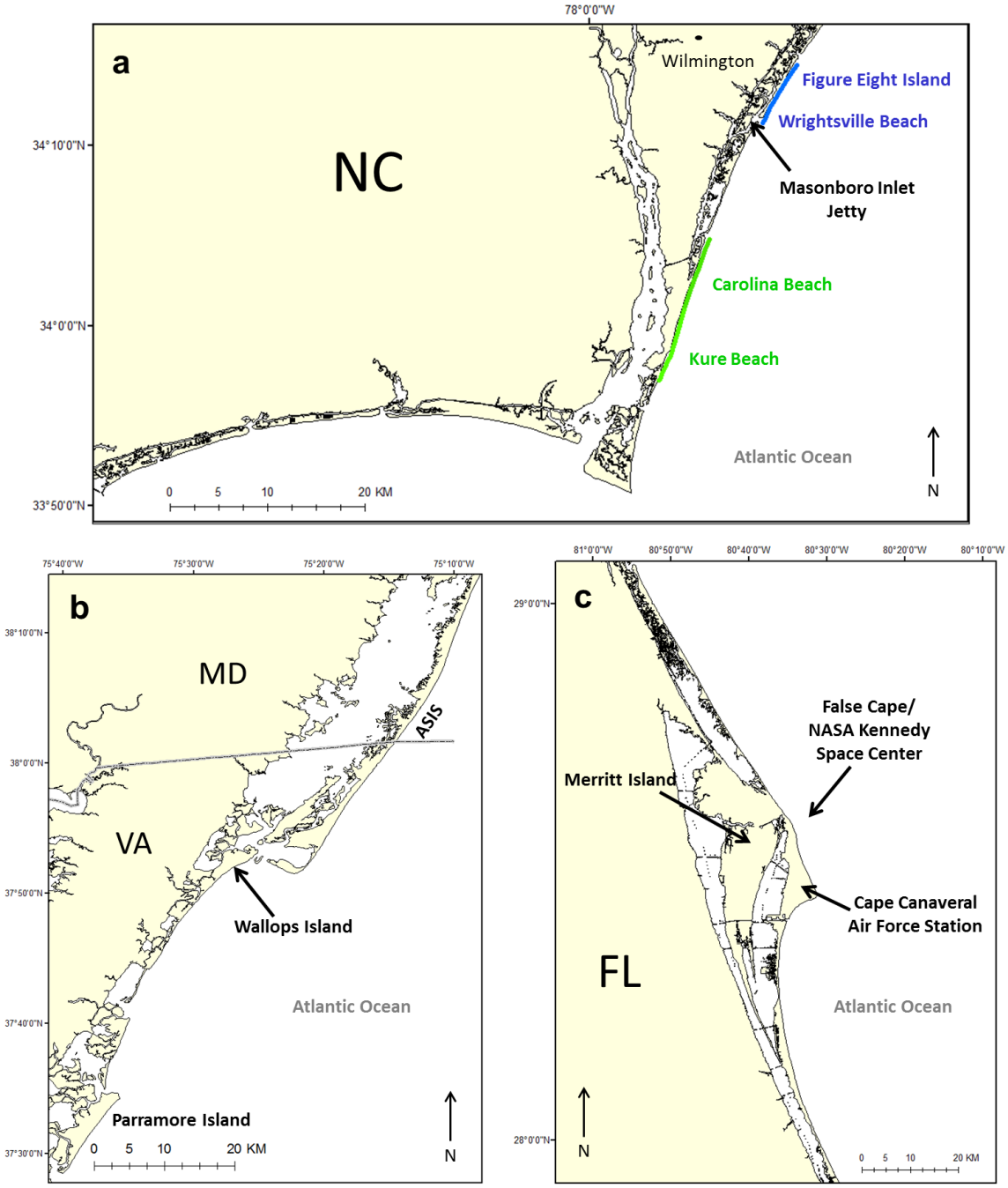

Figure 2. Detailed maps of study locations. (a) Cape Fear, North Carolina, USA. Kure Beach (KB) & Carolina Beach (CB) are locations of significant nourishment along the northern flank, approximated as Town 2 in model simulations while Town 2 represents the regions near Wrightsville Beach (WB), and Figure Eight Island (F8). (b) Fishing Point, MD & VA with the location of rotational Parramore Island, Assateague Island National Seashore (ASIS) and Wallops Island, home to NASA's Goddard Spaceflight Facility. (c) Cape Canaveral, FL, home to Cape Canaveral Air Force Station. The shoreline perturbation known as False Cape lies just north of Cape Canaveral and is the location of NASA's Kennedy Space Center. These areas are backed by Merritt Island.

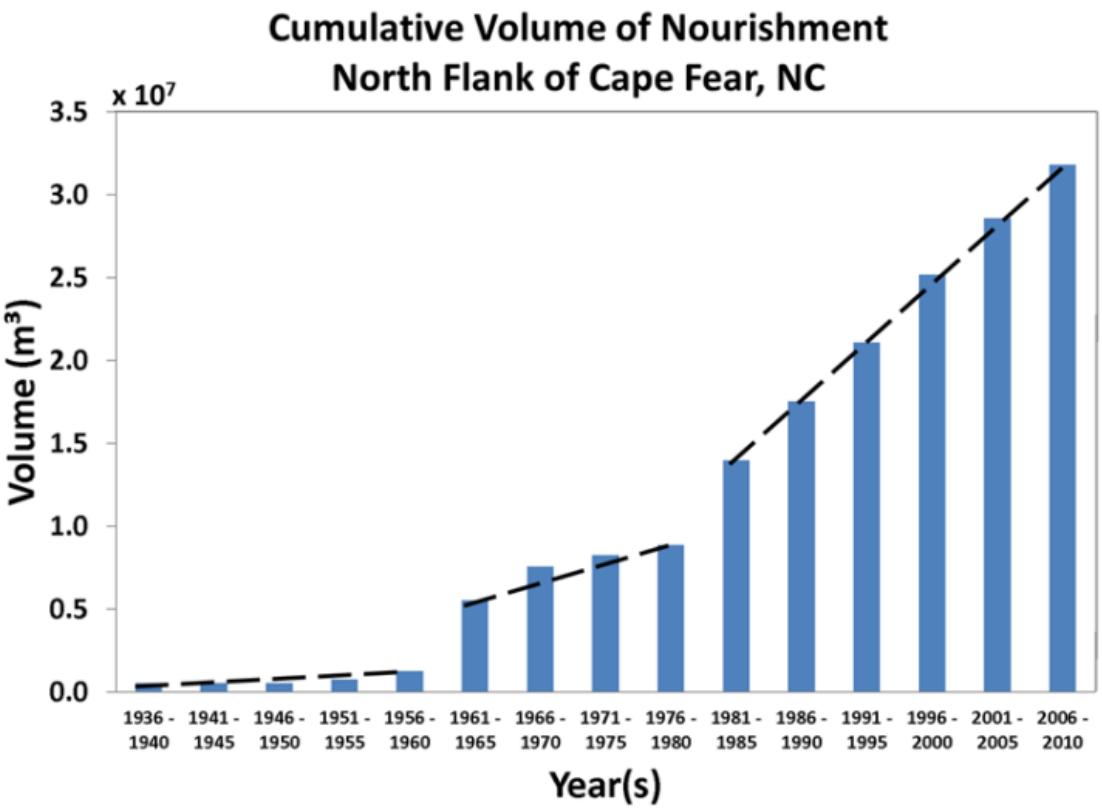

Figure 3. Cumulative beach nourishment volume for the northern flank of Cape Fear binned into 5-year increments. Three different rates of nourishment are indicated by dashed, black lines.

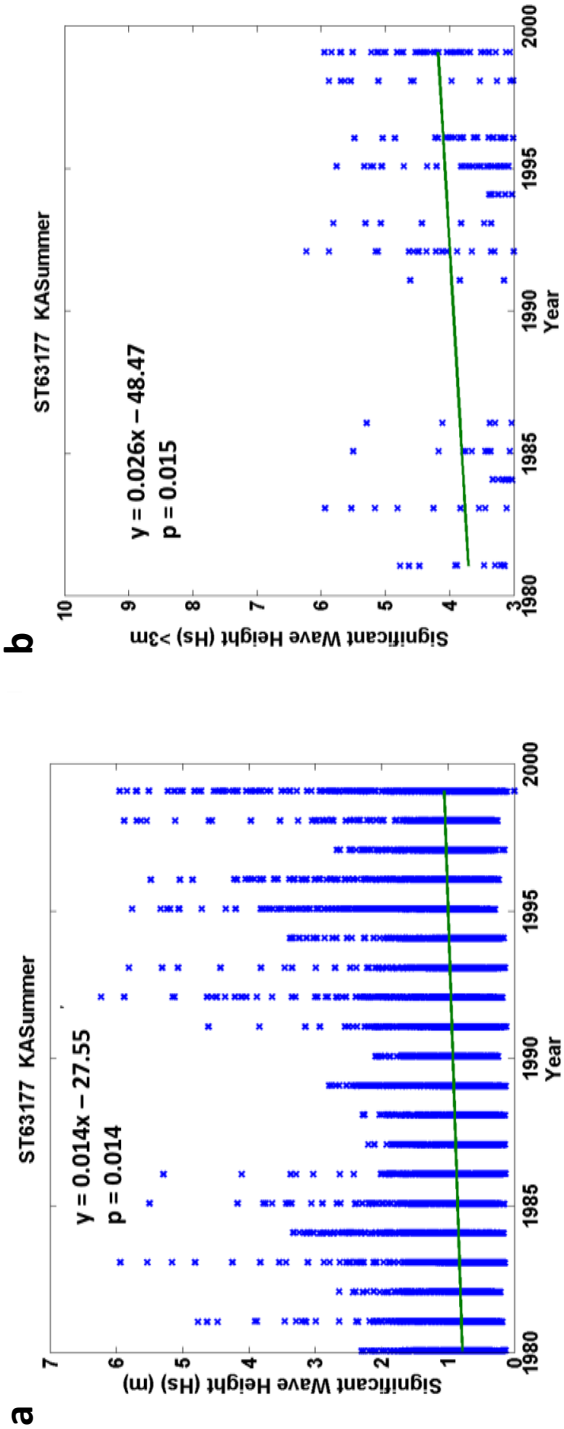

Figure 4. Representative plot of (a) increases in summer season significant wave height and (b) hurricane-generated waves off the coast of Fishing Point, MD & VA. Trends are significant at the 95% confidence level using the Wilcoxon rank-sum test.

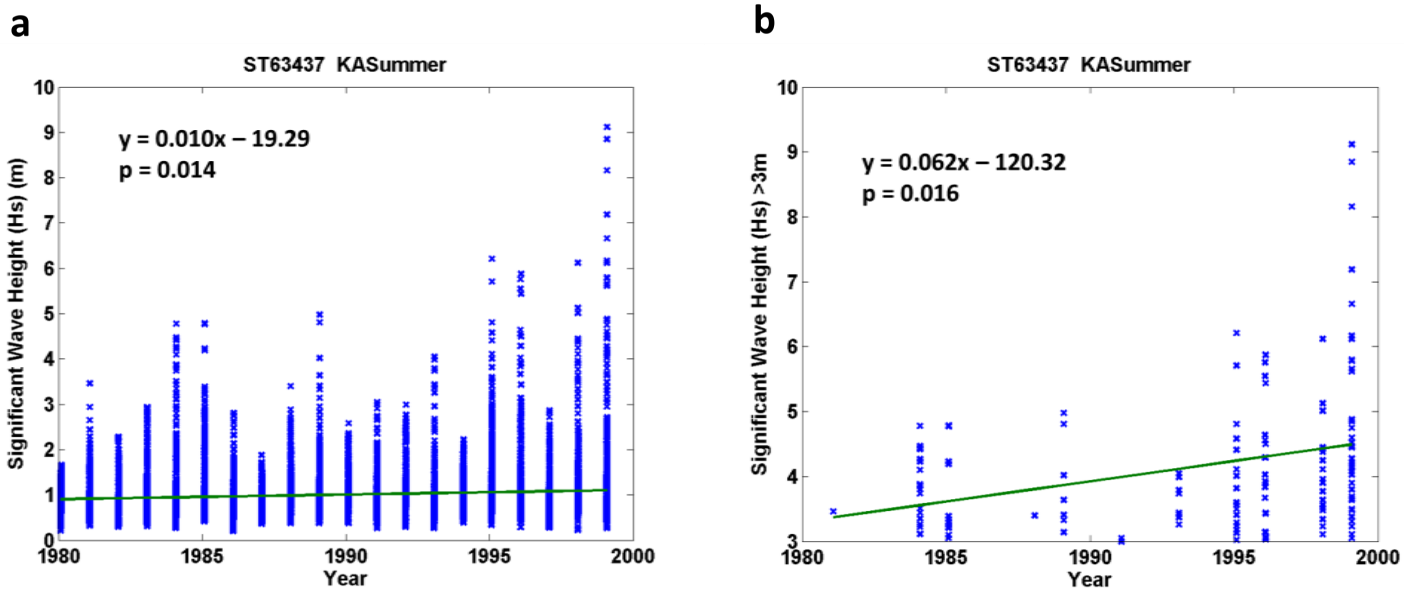

Figure 5. . Representative plot of (a) increases in summer season significant wave height and (b) hurricane-generated waves off the coast of Cape Canaveral, FL. Trends are significant at the 95 confidence level using the Wilcoxon rank-sum test.

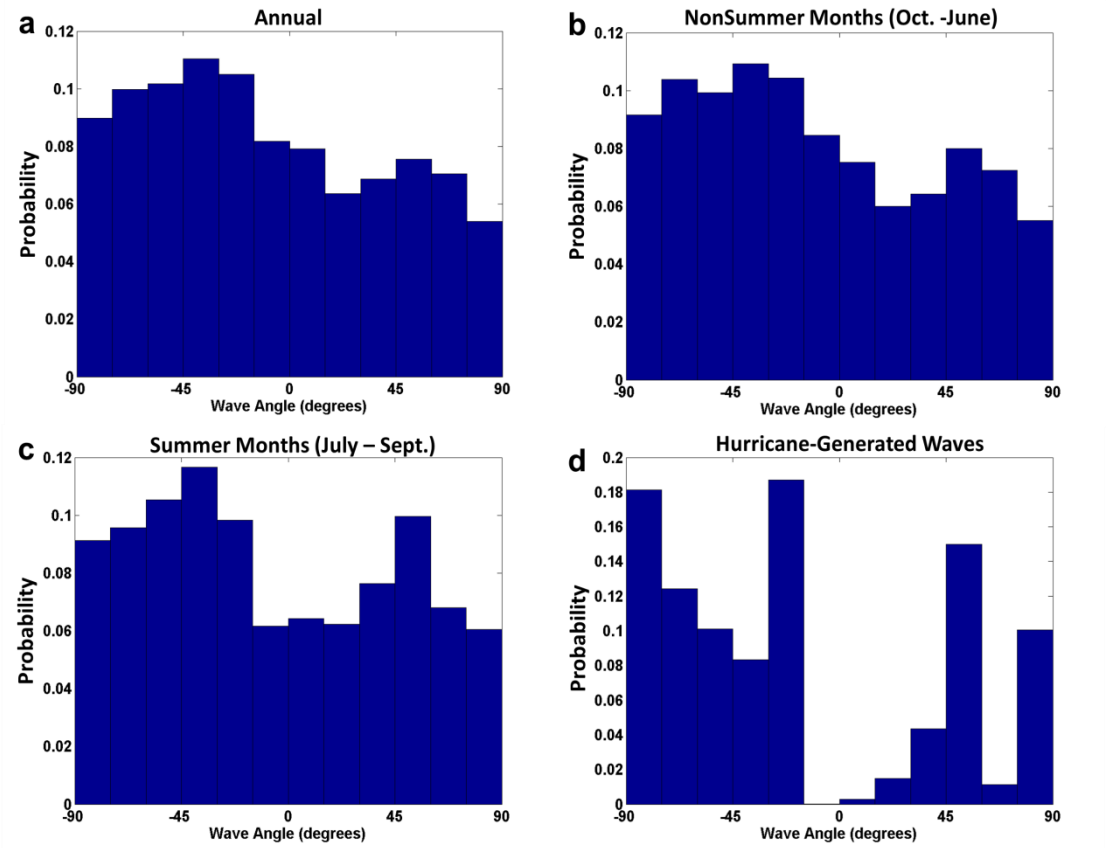

Figure 6. Representative wave climates off the coast of Fishing Point from WIS station 63177. Overall wave climate (a) and the non-summer wave climate (b) are bimodal with a high influence of waves from the left (north). (c) In the summer, the distribution becomes more bimodal and there is a greater influence of waves from the south. Hurricane-generated waves (d) approach from predominantly high angles (i.e., from northeast/east and south).

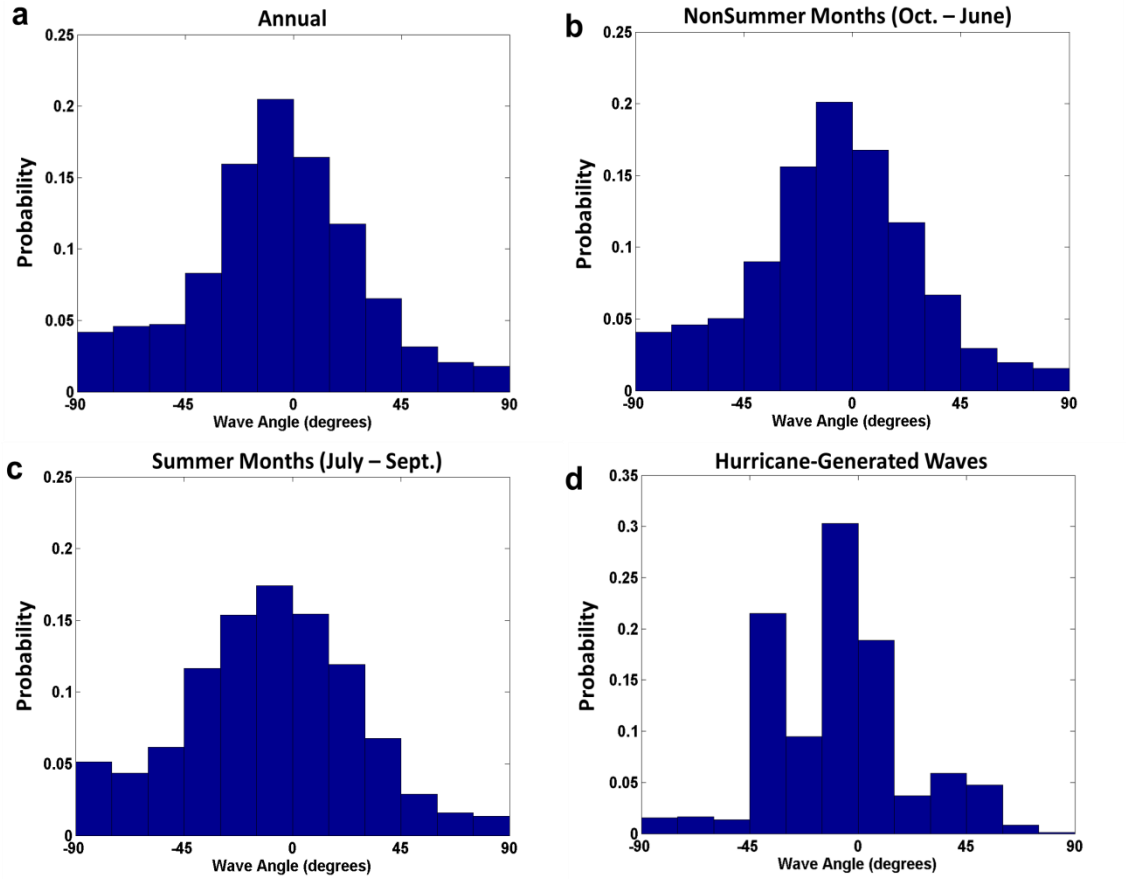

Figure 7. Representative wave climate in the vicinity of Cape Canaveral based on WIS Station 63437. The annual wave climate (a) and non-summer wave climate (b) are dominantly low-angle and slightly asymmetric, with a greater influence of waves approaching from the left (north relative to the general shoreline trend). Summer season waves (c) have an increased asymmetry with more waves approaching from the left (north) relative to other months of the year, and the hurricane-generated waves (those > 3m) (d) appear to approach from low-angles and the left (east).

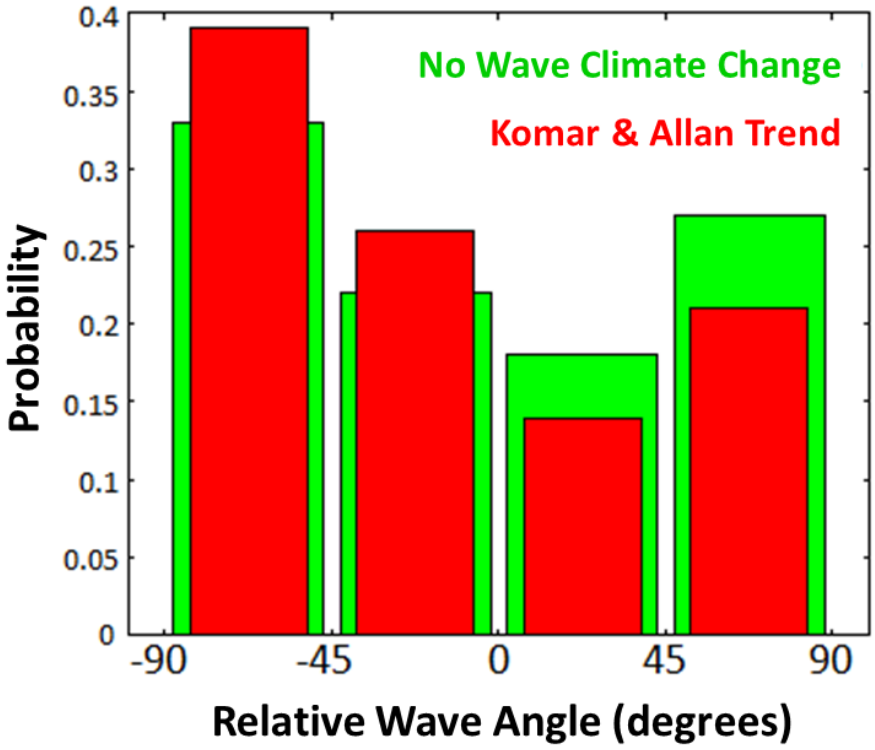

Figure 8. Wave climate probability distribution functions (of wave angle relative to general shoreline trend) used in model simulations. Green bins are distributions approximatebased on WIS hindcast data and red bins represent a wave climate reflective of observations by Komar & Allan (2008).

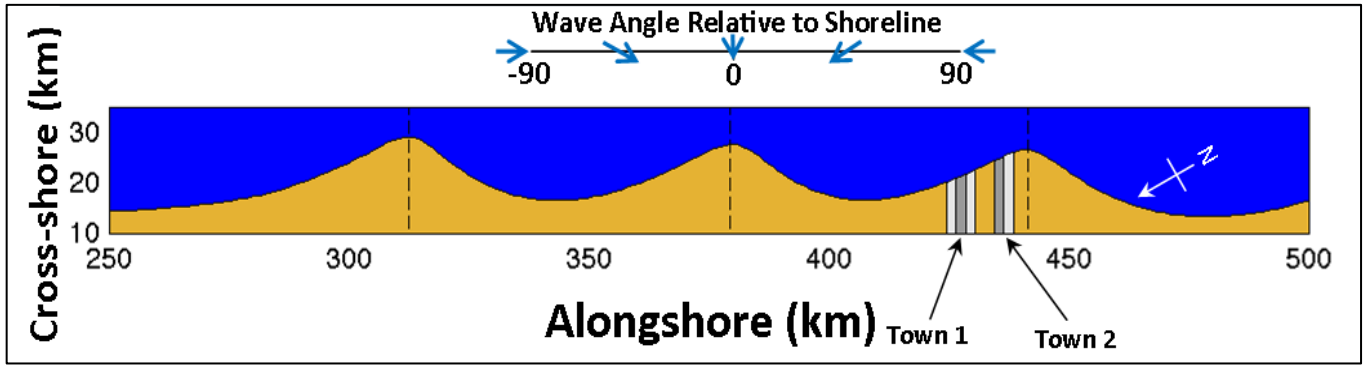

Figure 9. Schematic diagram of the model domain used for simulations including nourishment. Placement of Town 1 and Town 2 approximate locations having a long history of nourishment.

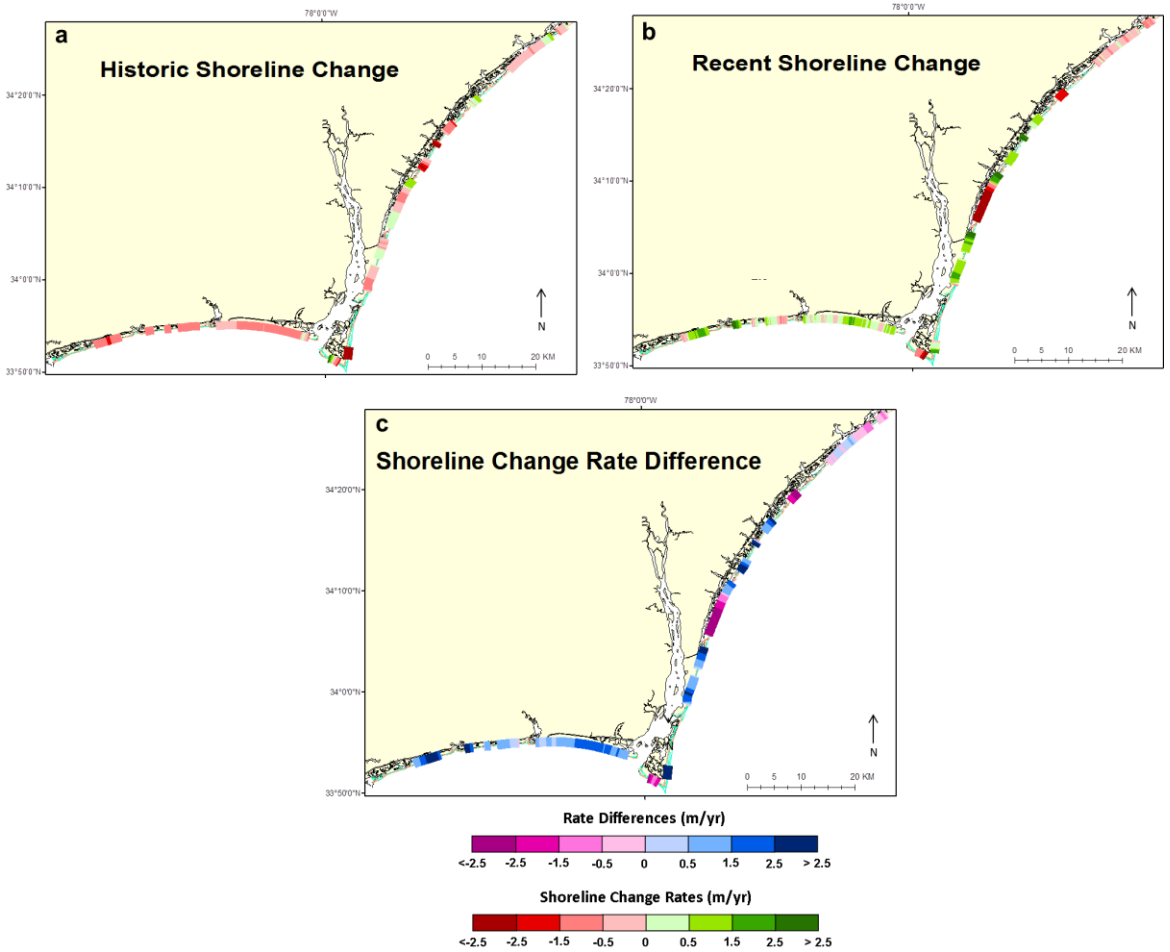

Figure 10. Shoreline change analysis for Cape Fear, NC. Shoreline change rates for (a) historic and (b) recent time periods. Reds represent negative (erosional) rates while greens are positive (accretional) values. Shoreline change rate difference (c), calculated by subtracting historic rates from the recent rates. Blues indicate areas that have become increasingly accretional in the recent while purples and pinks areas have become increasingly erosional

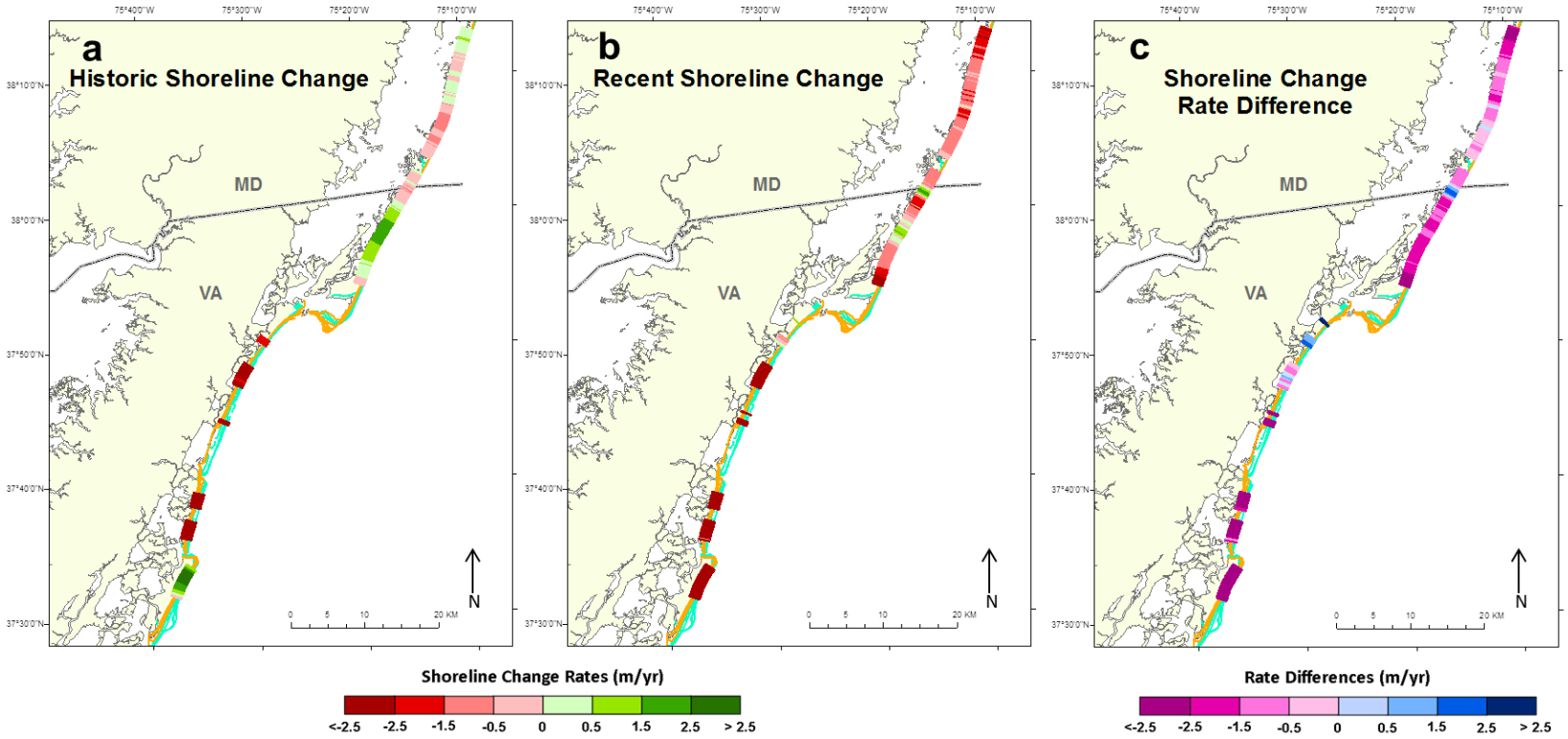

Figure 11. Shoreline change analysis for Fishing Point, MD&VA. Colors represent same values as in Fig. 5.

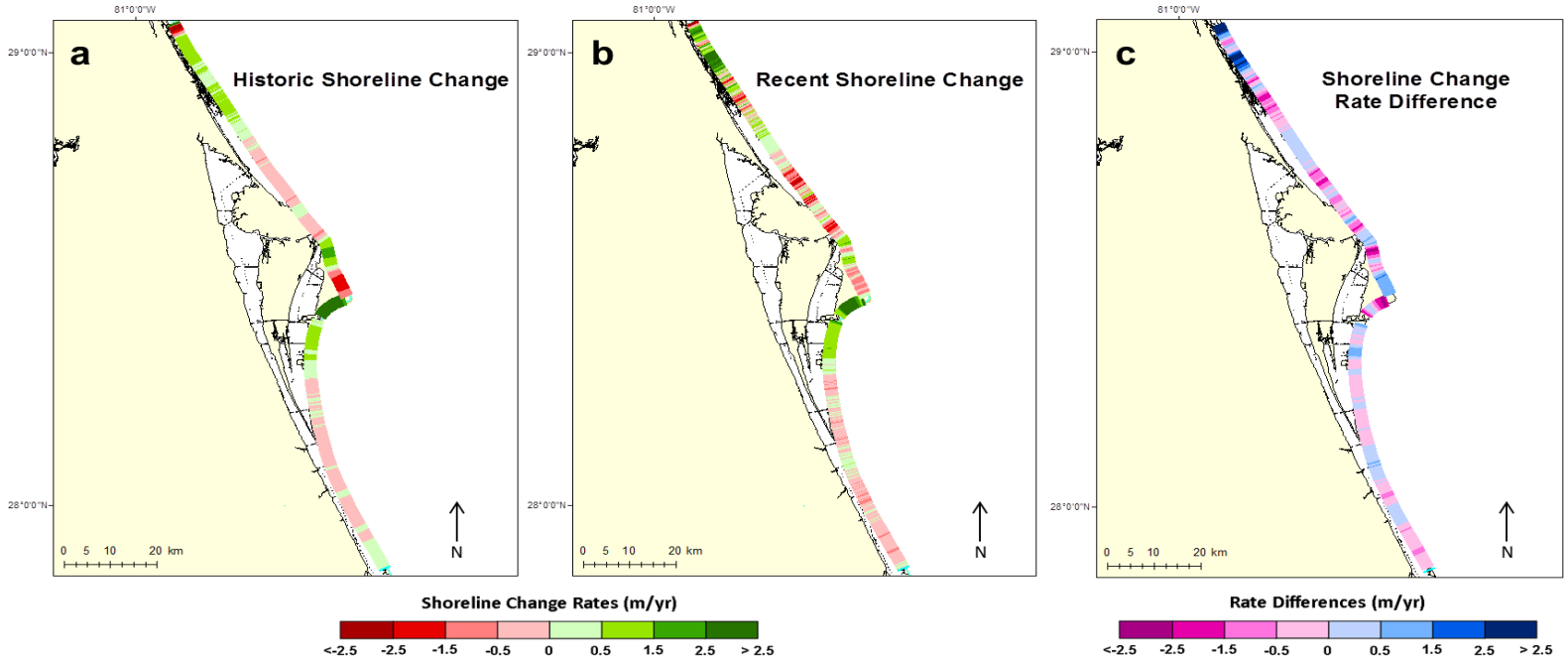

Figure 12. Shoreline change analysis for Cape Canaveral, FL. Colors represent same values as in Fig. 5.

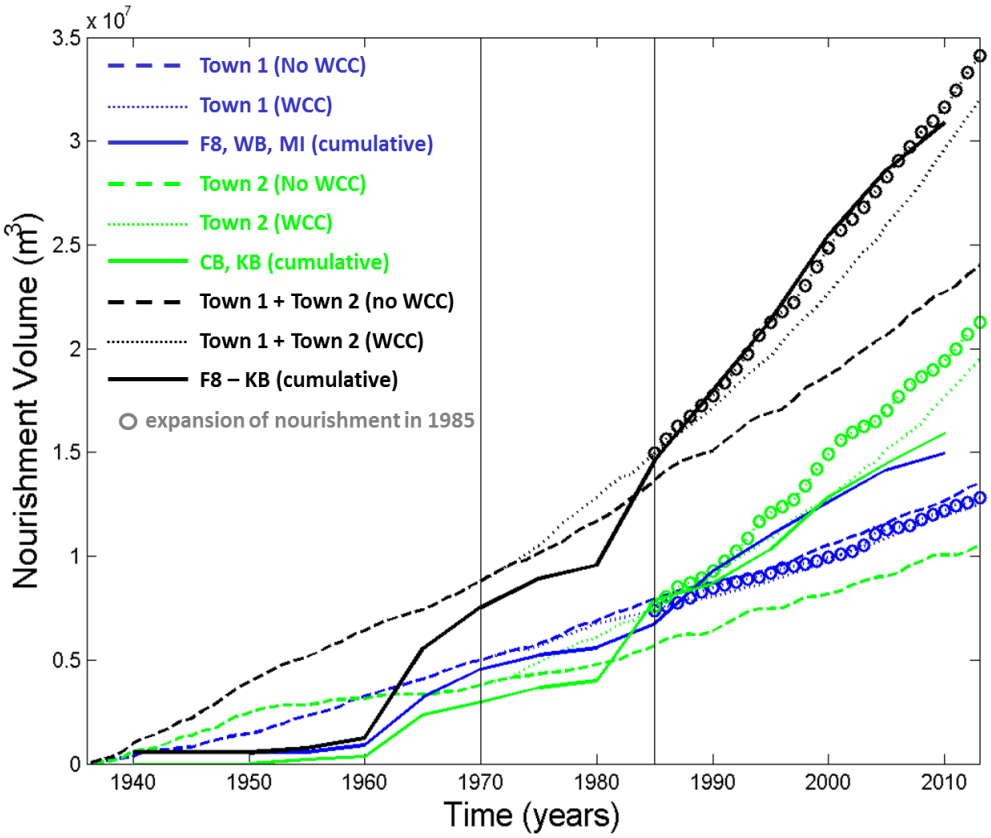

Figure 13. Observed and model-generated cumulative nourishment volumes for the north flank of Cape Fear. Solid black line represents observations of combined nourishment from Figure Eight Island (F8) south to Carolina Beach (CB). The dashed and dotted lines represent model-generated nourishment volumes for Town 1 without wave climate change (No WCC) and with wave climate change (WCC). Carolina Beach (CB) and Kure Beach (KB) nourishment observations are shown in the solid green line while the dashed and dotted green lines represent model runs with no WCC and with WCC, respectively. The dotted lines with circles overlain represent model runs with WCC and expansion of nourishment after 1985. The vertical lines at 1970 and 1985 reflect the onset of wave climate change and expansion of nourishment respectively.

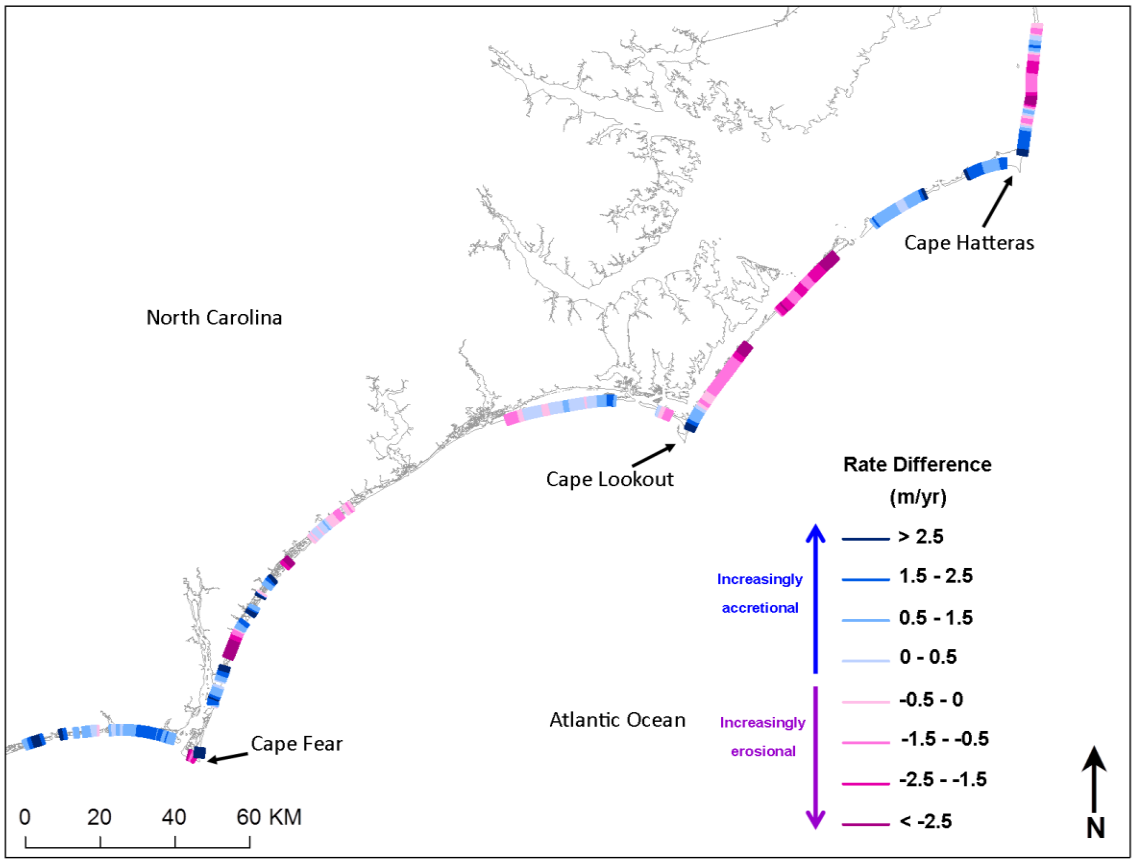

Figure 14. Shoreline change rate differences (SCRDs) for all three North Carolina SCRDs for Cape Hatteras and Cape Lookout indicate the northern flanks have become more erosional/less accretional whereas the southern flanks have become more accretional/less erosional. In contrast, Cape Fear lacks the same erosional signal on the northern flank, with the exception of an area known to have relatively little beach nourishment activity. Data for Cape Hatteras and Cape Lookout from Moore et al. (in review).

Cape Fear Shorelines				
Year(s)	**Source Agency**	**Original Media**	**Shoreline Datum/Proxy**	**Extent**
Historic:				
1849 – 1873	USGS	T-sheets/CERC maps	HWL	F
1877 – 1878	NOAA	T-sheets	Nat. MHWL	P
1914	NOAA	T-sheets	Nat. MHWL	P
1933 – 1934	USGS	T-sheets	HWL	F
1936 – 1937	NOAA	T-sheets	Nat. MHWL	P
1942 – 1944	USGS	T-sheets	Nat. MHWL	P
1962 – 1969	NOAA	T-sheets	Nat. MHWL	P
Recent:				
1970-1973	USGS	T-sheets/CERC maps	HWL	F
1997	USGS	LiDAR survey	LiDAR MHWL	F
1998	NC DENR	Aerial Photos	Wet-Dry Line	F
2003	NC DENR	Aerial Photos	Wet-Dry Line	F
2004	NC DENR	Aerial Photos	Wet-Dry Line	F

Table 1. Cape Fear shoreline information

Fishing Point Shorelines				
Year(s)	**Source Agency**	**Original Media**	**Shoreline Datum/Proxy**	**Extent**
Historic:				
1849 -1852	USGS	T-sheet	HWL	F
1859 - 1887	USGS	T-sheet	HWL	P
1908 - 1910	USGS	T-sheet	HWL	P
1933	USGS	T-sheet	HWL	P
1942 -1943	USGS	T-sheet	HWL	F
1962	USGS	T-sheet	HWL	F
Recent:				
1980	USGS	Air Photo	HWL	P
1989	USGS/MD DNR	T-sheets	HWL	P
1995	ASIS	GPS	Wet-dry Line	P
1997	ASIS/Oster (2012)	GPS/LiDAR	Wet-dry line/LiDAR MHWL	F
1998	ASIS/Oster (2012)	GPS/LiDAR	Wet-dry line/LiDAR MHWL	F
2005	ASIS/Oster (2012)	GPS/LiDAR	Wet-dry line/LiDAR MHWL	F
2009	ASIS/Oster (2012)	GPS/LiDAR	Wet-dry line/LiDAR MHWL	F
2010	ASIS	GPS	Wet-dry Line	P

Table 2. Fishing Point shoreline information. None of the USGS shorelines contained information, either in attribute tables or metadata that indicated what shoreline datum/proxy was used to delineate the shoreline. MD DNR – Maryland Department of Natural Resources.

Cape Canaveral Shorelines				
Year(s)	**Source Agency**	**Original Media**	**Shoreline Datum/Proxy**	**Extent**
Historic:				
1851 - 1884	USGS	T-sheets/CERC maps	HWL	F
1923 - 1930	USGS	T-sheets/CERC maps	HWL	F
1943	NAPP/NASA	Aerial Plates/Rescanned	Wet-dry line	P
1948	NOAA	Aerial Photos	Nat. MHWL	P
1951	NAPP/NASA	Aerial Plates/Rescanned	Wet-dry line	P
1958	NAPP/NASA	Aerial Plates/Rescanned	Wet-dry line	P
1964	NOAA	Aerial Photos	Nat. MHWL	P
1966 -1967	NOAA	Aerial Photos	Nat. MHWL	F
Recent:				
1969 - 1970	NOAA	Aerial Photos	Nat. MHWL	P
1994	NAPP	Aerial Photos	Wet-dry line	P
1999	USGS	LiDAR	LiDAR MHWL	F
2000	Kucera Int.	Aerial Photos	Wet-dry line	P
2002	DigitalGlobe, Inc.	Ikonos	Wet-dry line	P
2003	NAPP	Aerial Photos	Wet-dry line	P
2004	FFand W	Aerial Photos	HWL	F
2005	FL DOT	Aerial Photos	Wet-dry line	P
2006	FL DEP	Aerial Photos	Wet-dry line	P
2007	Arieals Express Inc.	Aerial Photos	Wet-dry line	P
2009	DigitalGlobe, Inc.	Geoeye 1	Wet-dry line	P
2010	DigitalGlobe, Inc.	Geoeye 1	Wet-dry line	P

Table 3. Cape Canaveral shoreline information. NAPP- National Aerial Photography Program, NASA – National Aeronautics and Space Administration, Ikono is a DigitalGlobe satellite with a 1m resolution, Geoeye 1 is a DigitalGlobe satellite with a 0.5m resolution.

Appendices

Appendix A. Extent of LRRs & EPRs

DSAS can calculate linear regression rates (LRRs) for transects that intersect a minimum of 3 shorelines. However, there are significant portions of my study areas where only two shorelines are available for a given time period. If only one shoreline is available, no shoreline change can be calculated. However, if I have two shorelines, the end-point rate (EPR) method can be used to measure shoreline change. Each method of rate calculation is widely used and accepted in the coastal science community (Dolan et al., 1991). For Cape Fear, NC, the historic time period had a significant portion of the northern flank with only two shorelines available and thus a

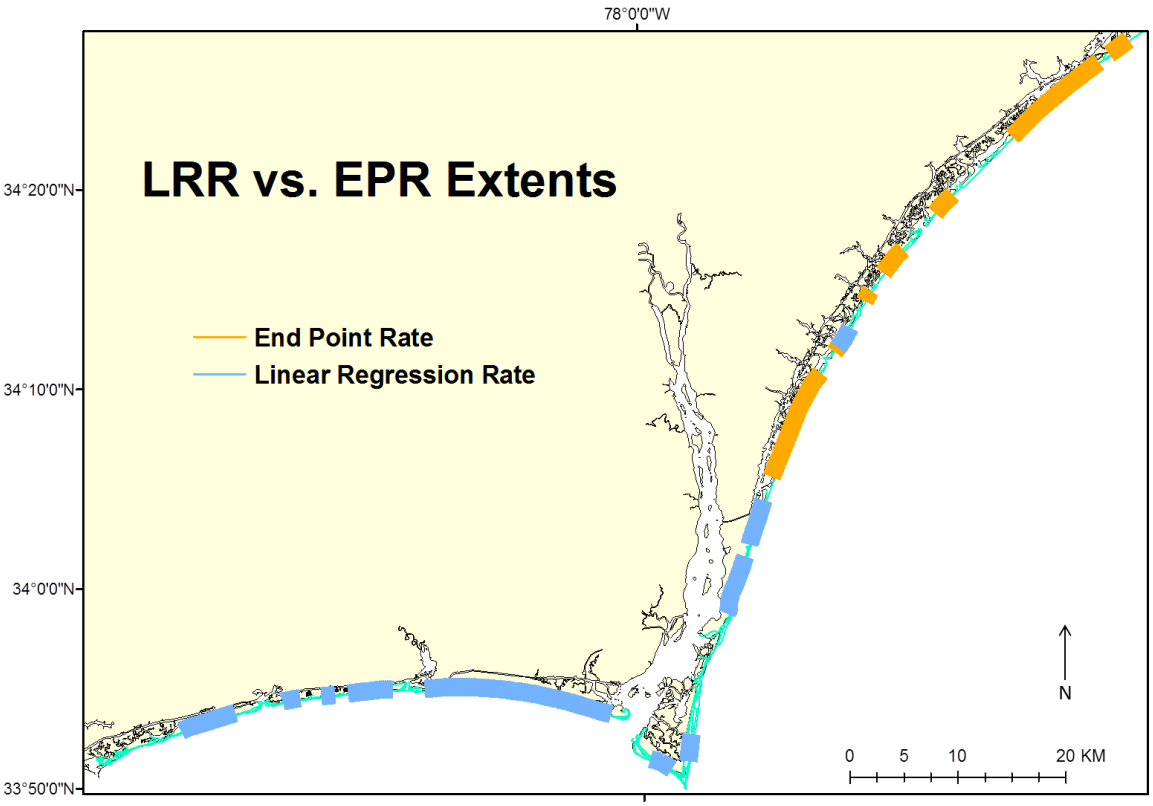

Figure 1. Extent of LRRs vs. EPRs along Cape Fear, NC used in historic shoreline change analysis.

significant portion with EPR calculations (Fig. 1).Shorelines used for these EPR calculations are the 1849–1873 & 1933-1944 shorelines.

These two shorelines are spaced far enough apart temporally that the coverage they provide is sufficient for characterization of the shoreline change in the historic time period. This results in 60% of transects with a LRR calculated, and 40% with EPRs.

At Fishing Point there were enough historic shorelines that no EPRs needed to be calculated. For the recent time period, very few EPRs were needed (95% LRRs, 5% EPRs) (Fig.

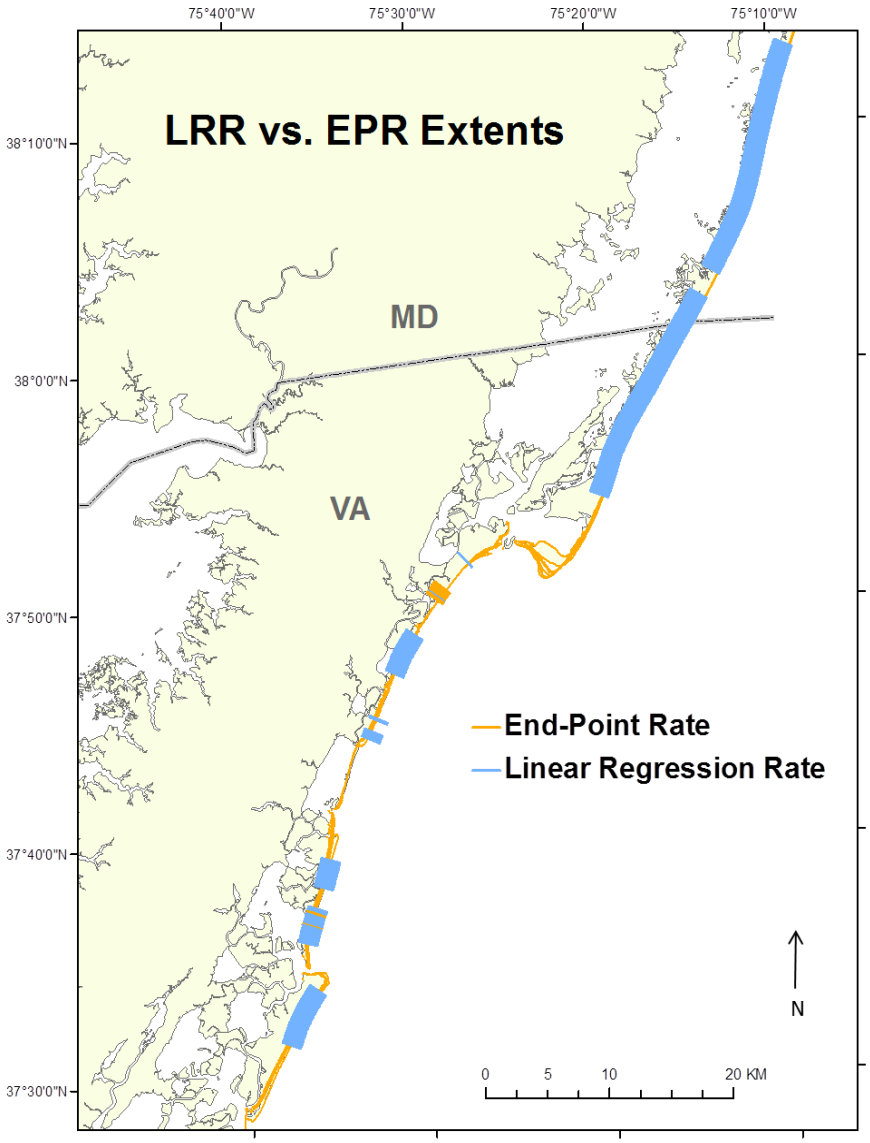

Figure 2. Extent of LRRs vs. EPRs along Fishing Point, MD & VA used in recent shoreline change analysis

2).

Analysis of Cape Canaveral required EPR calculations along the northernmost extent of the study area for both historic and recent time periods. In the historic time period, the two shorelines used were from 1851-1884 & 1923 – 1930 and in the recent shoreline available were 1999 and 2004. While both time periods have approximately 72% LRRs and 28% EPRs (Fig. 3), from the historic to the recent an area of LRRs shifted northward, while some EPR calculations shifted south.

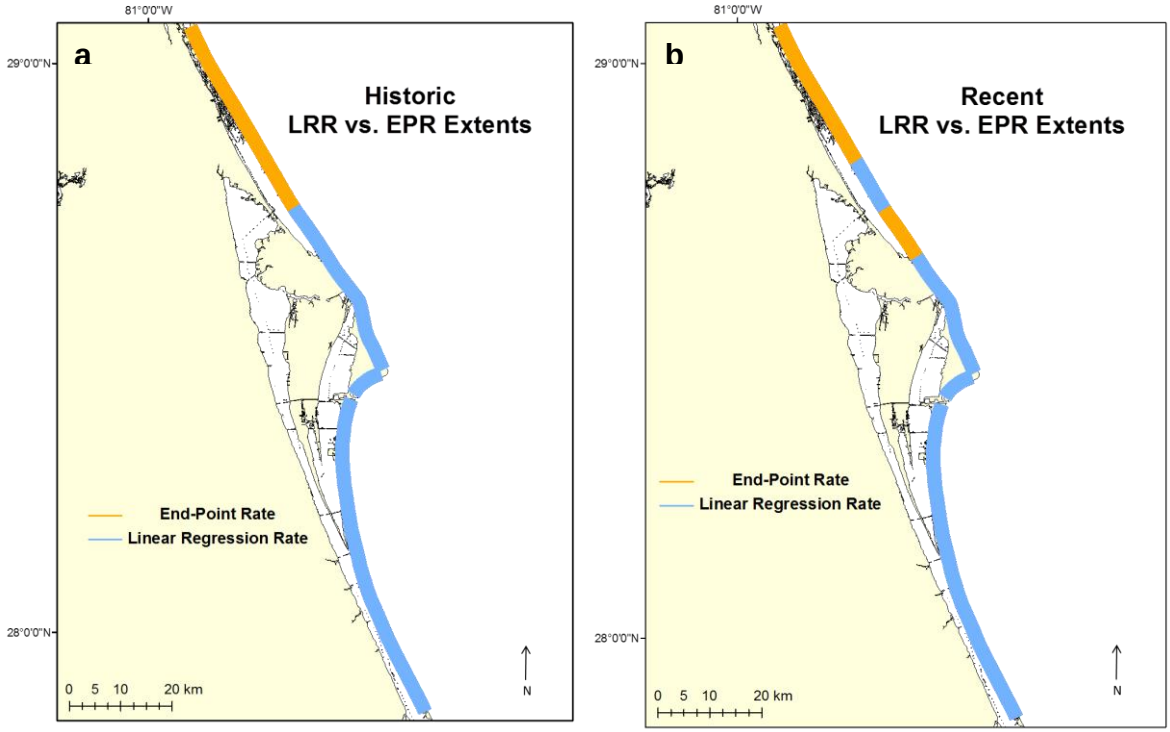

Figure 3. Extent of LRRs vs. EPRs along Cape Canaveral, FL used in (a) historic shoreline change analysis and (b).recent shoreline change analysis

Appendix B. Nourishment Data & Graphs

To determine the best method for modeling nourishment along the northern flank of Cape Fear, I wanted to examine the relative amounts of nourishment in each community as compared to other communities throughout time. While the alongshore distribution of nourishment during each episode can vary, I had to select one representative community length in order to find normalized nourishment volumes per meter of shoreline. Thus, I selected the longest alongshore

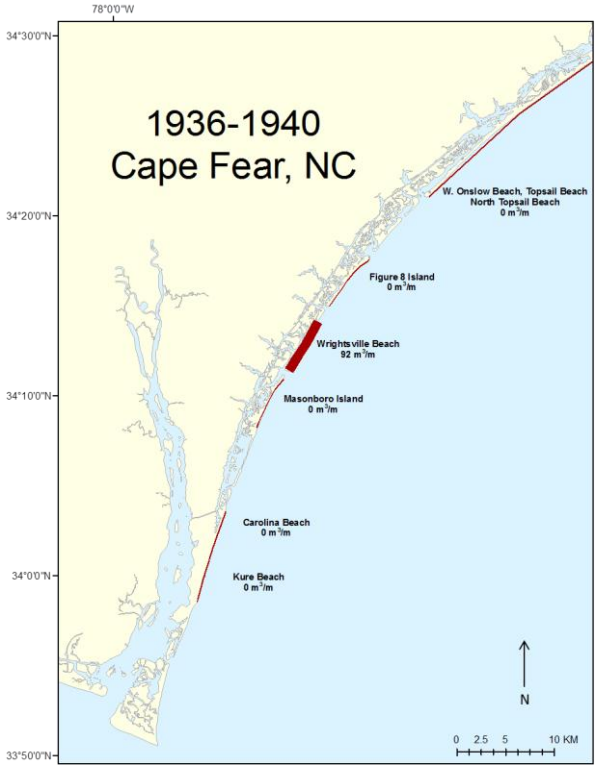

Figure 1. Map of nourishment volumes along the northern flank of Cape Fear. Volumes have been normalized to alongshore community length for each community from 1936 – 1940. Line width reflects relative nourishment through time.

length of nourishment given for each community in the PSDS (2012) data for communities from Kure Beach north was selected and used to normalize nourishment per community for each 5-year period.

After normalizing the nourishment volumes through time, I found the two communities of Wrightsville Beach and Carolina/Kure Beach contributed the largest volumes and nourished most consistently throughout this record. There also appears to be an increase in the spatial extent of larger nourishment episodes beginning around 1985. Based upon this, I selected two town locations to approximate the locations of Wrightsville and Carolina/Kure Beach and initially restricted nourishment to small extents. Then, in 1985 I expanded the shoreline of the towns in order to reflect the observations of increased spatial extent of nourishment.

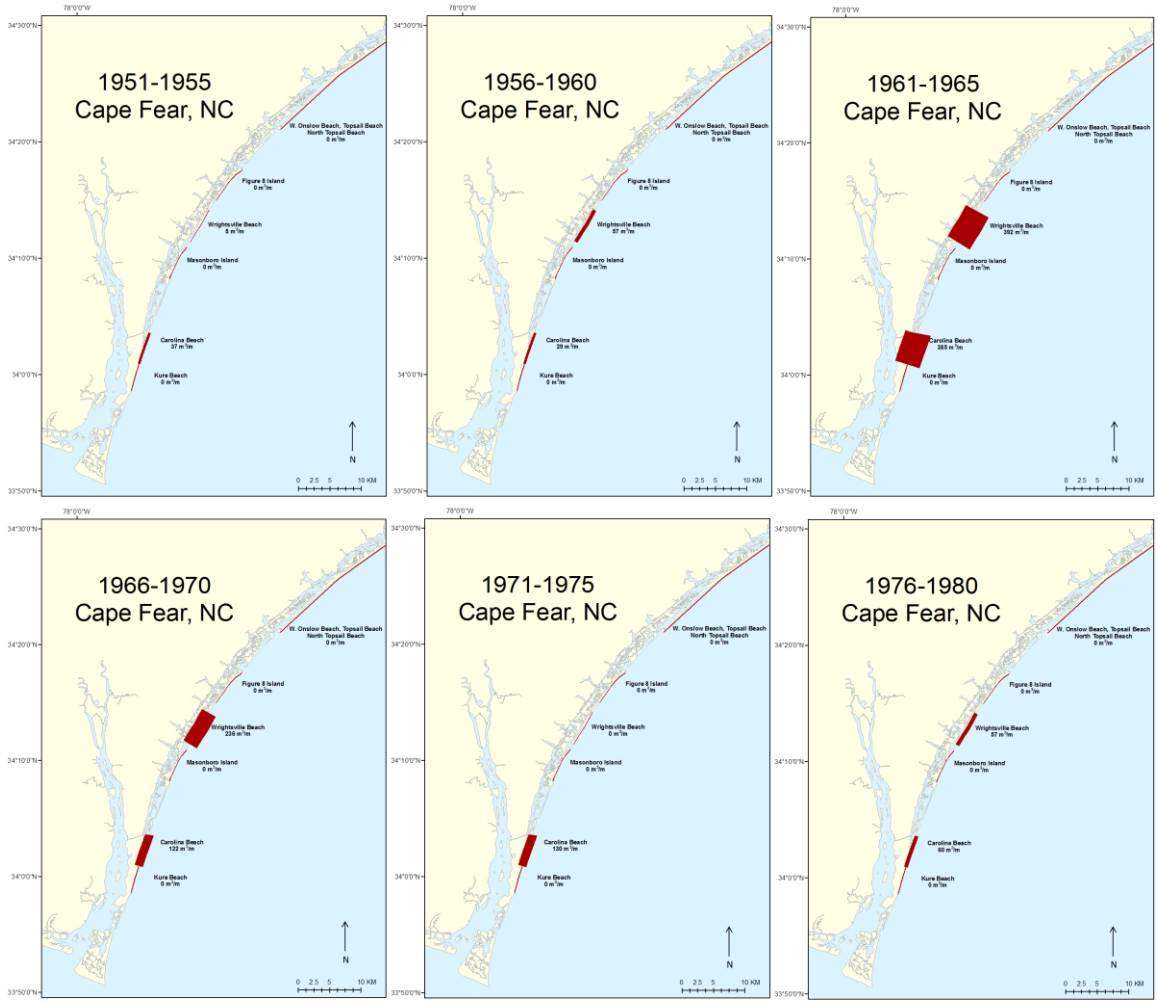

Figure 2. Maps of normalized nourishment volumes for each community broken in to 5 year bins. Line width reflects relative nourishment throughout time.

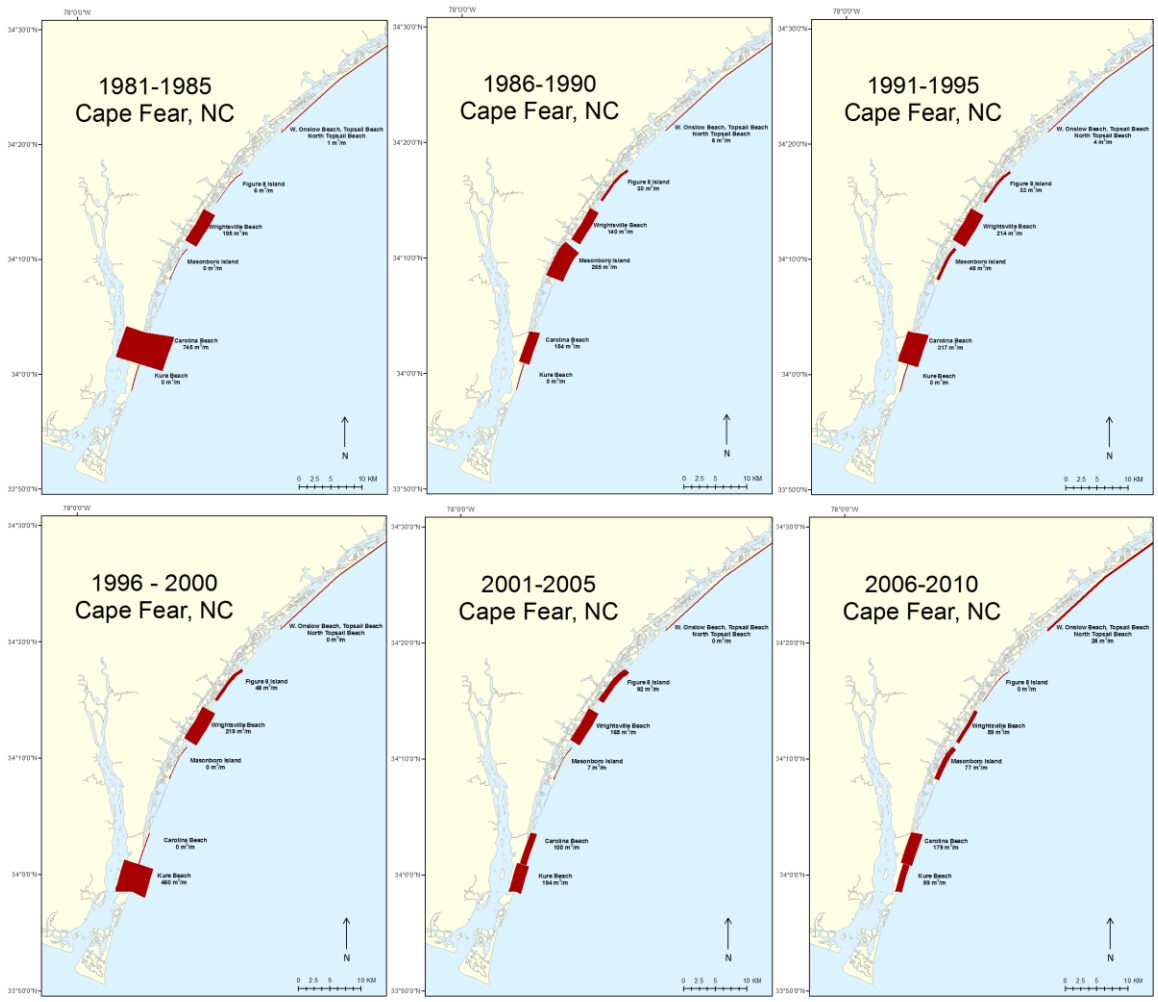

Figure 3. Maps of normalized nourishment volumes for each community, broken in to 5 year bins. Line width reflects relative nourishment throughout time.

Appendix C. Wave Climate Analysis

I established the seasonal contribution to significant wave height increases for the Cape Canaveral region. Data from 19 Wave Information Studies (WIS) stations were downloaded. 15 of those were shallow-water stations, while 4 stations are in deep water (Fig. 1). This was then broken into summer season (July-September) and all other months. A linear regression trend was calculated for both the significant wave heights and those with heights > 3m. All linear regressions are significant at the 95% confidence level using the Wilcoxon rank sum test.

For the summer season, shallow water buoys saw significant wave height increases that ranged from 0.004 m/yr to 0.12 m/yr over approximately 20 years (Fig. 2). Hurricane-generated wave heights increased by 0.4 to 0.74 m/yr (Fig. 3). Deep water buoys have similar increases, with 0.006m to 0.01 m/yr increases in all significant wave heights (Fig. 4) and 0.056 to 0.74 m/yr increases in hurricane-generated waves (Fig. 5). It is likely that the majority of increases in summer-season significant wave heights results from increases in the hurricane-generated wave heights.

Trends in significant wave heights for all other months of the year also have increasing trends, but these are lower increases. The shallow water buoys saw increases that range from 0.002 to 0.013 m/yr for significant wave heights (Fig. 6) and 0.02 to 0.3 m/yr for waves >3m (Fig. 7). Interestingly, the trend in deep water waves is very small and very close to zero, with ranges of 0.0068 to 0.0095 for all significant wave heights (Fig. 8)and 0.004 to 0.006 m/yr for waves >3m high (Fig. 9).

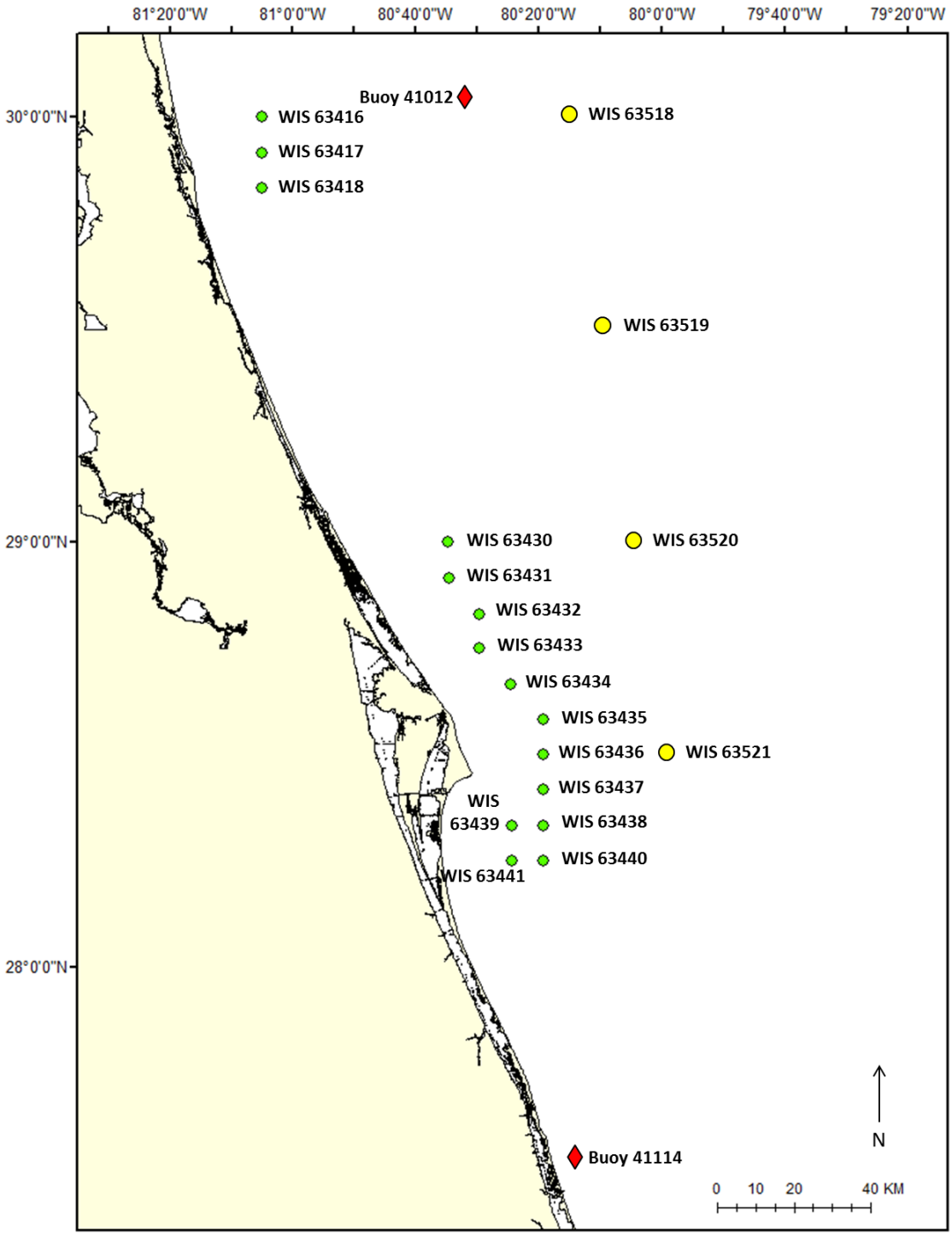

Figure1. Buoy and WIS station locations off the coast of Cape Canaveral. WIS station data can be downloaded from wis.usace.army.mil.

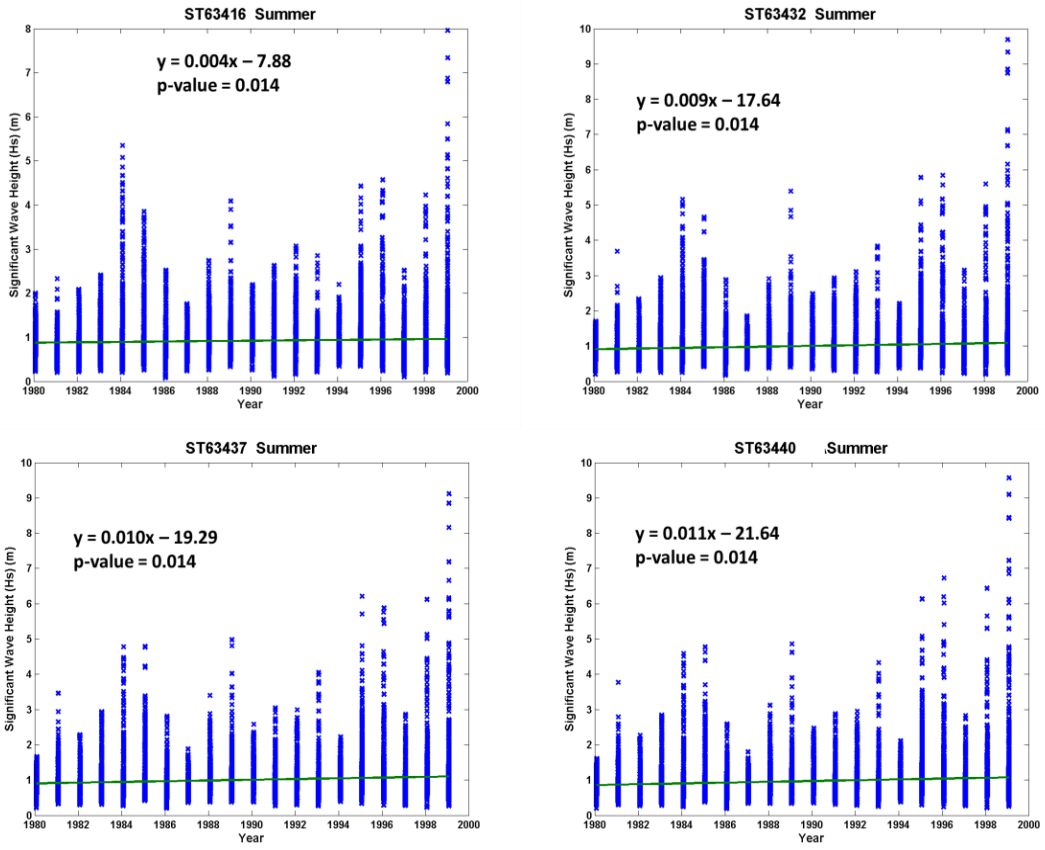

Figure 2. Summer season significant wave height and trends for shallow water WIS stations near Cape Canaveral, FL.

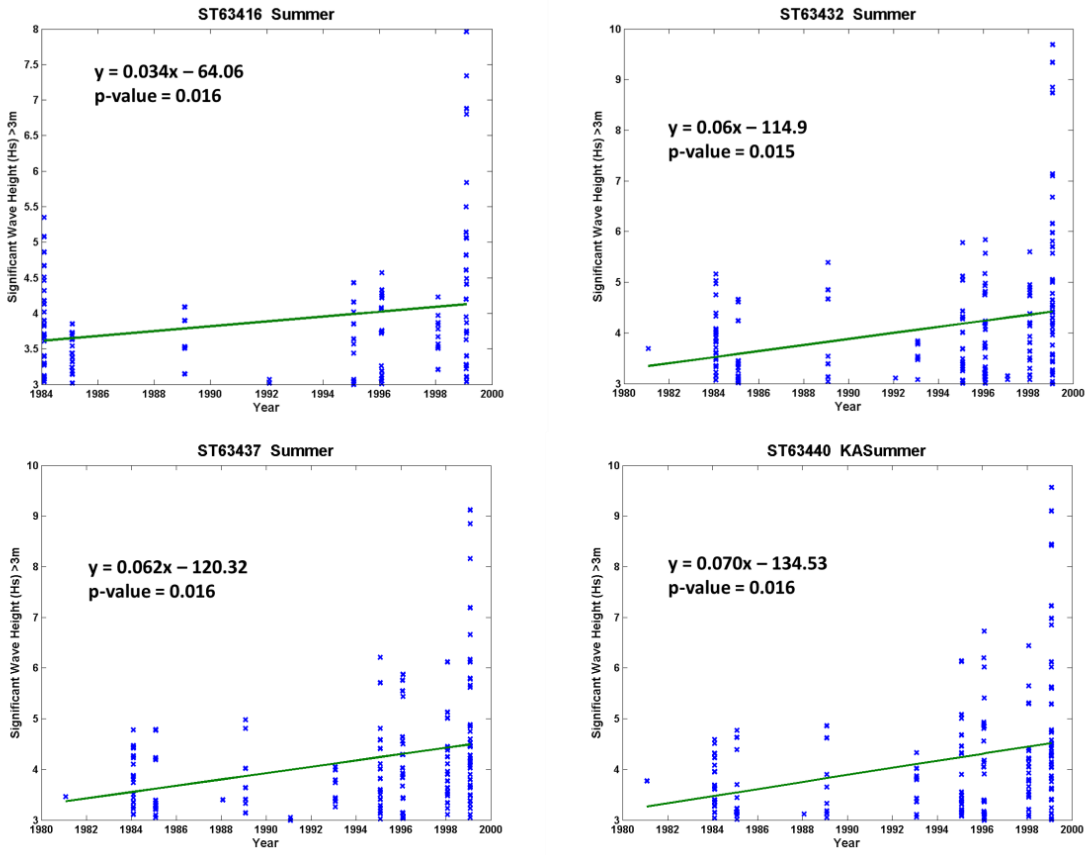

Figure 3. Hurricane-generated wave height and trends from shallow water WIS stations near Cape Canaveral, FL.

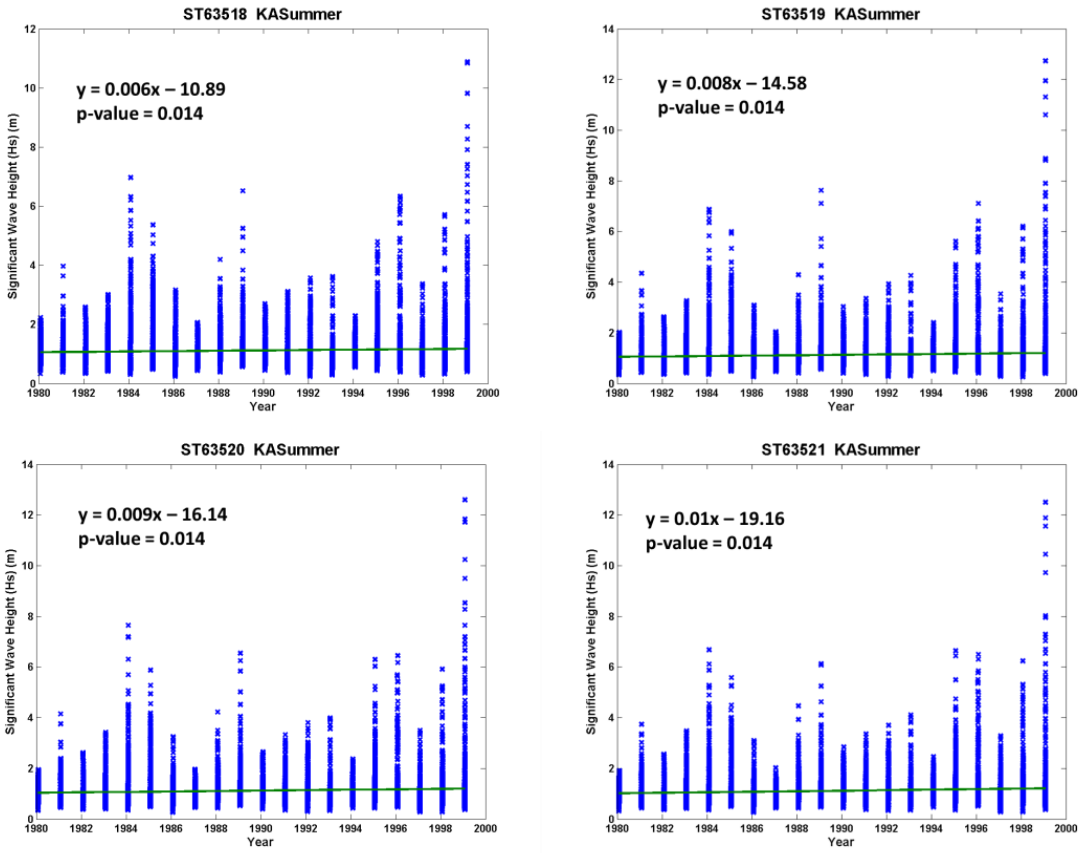

Figure 4. Summer season significant wave heights and trends for deep water WIS stations near Cape Canaveral, FL.

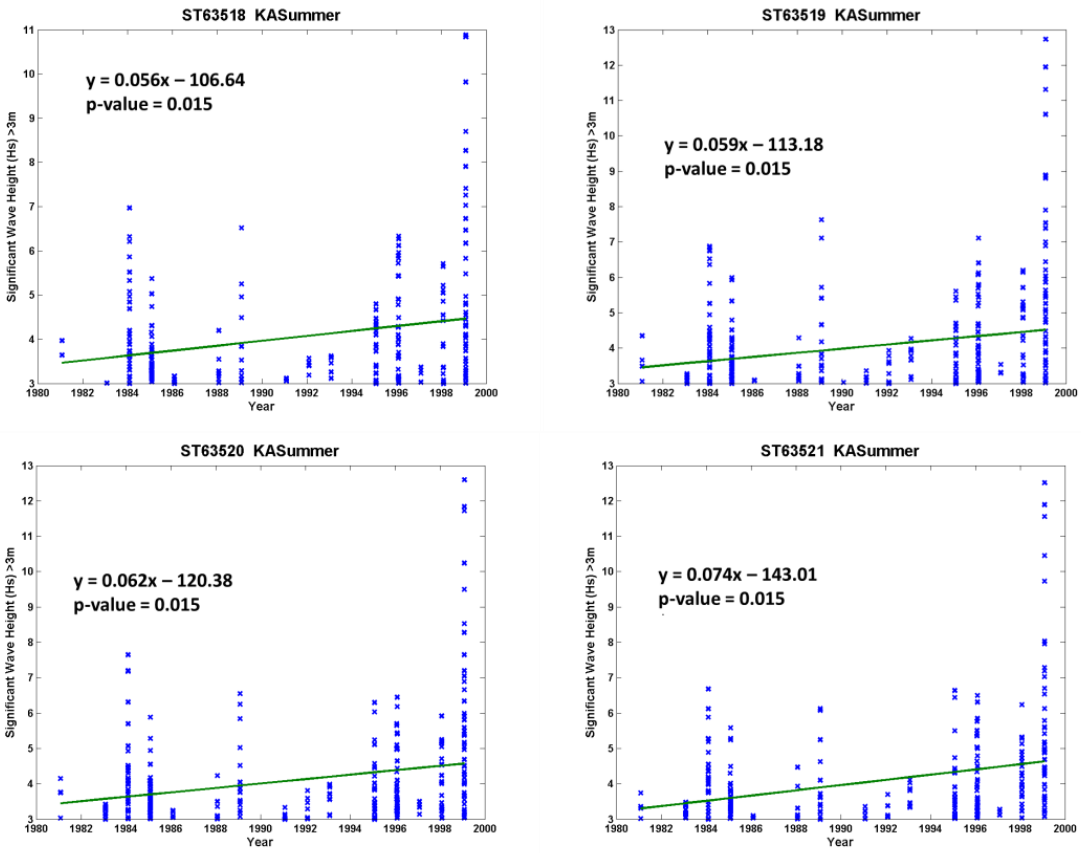

Figure 5. Hurricane-generated wave height and trends for deep water buoys near Cape Canaveral, FL.

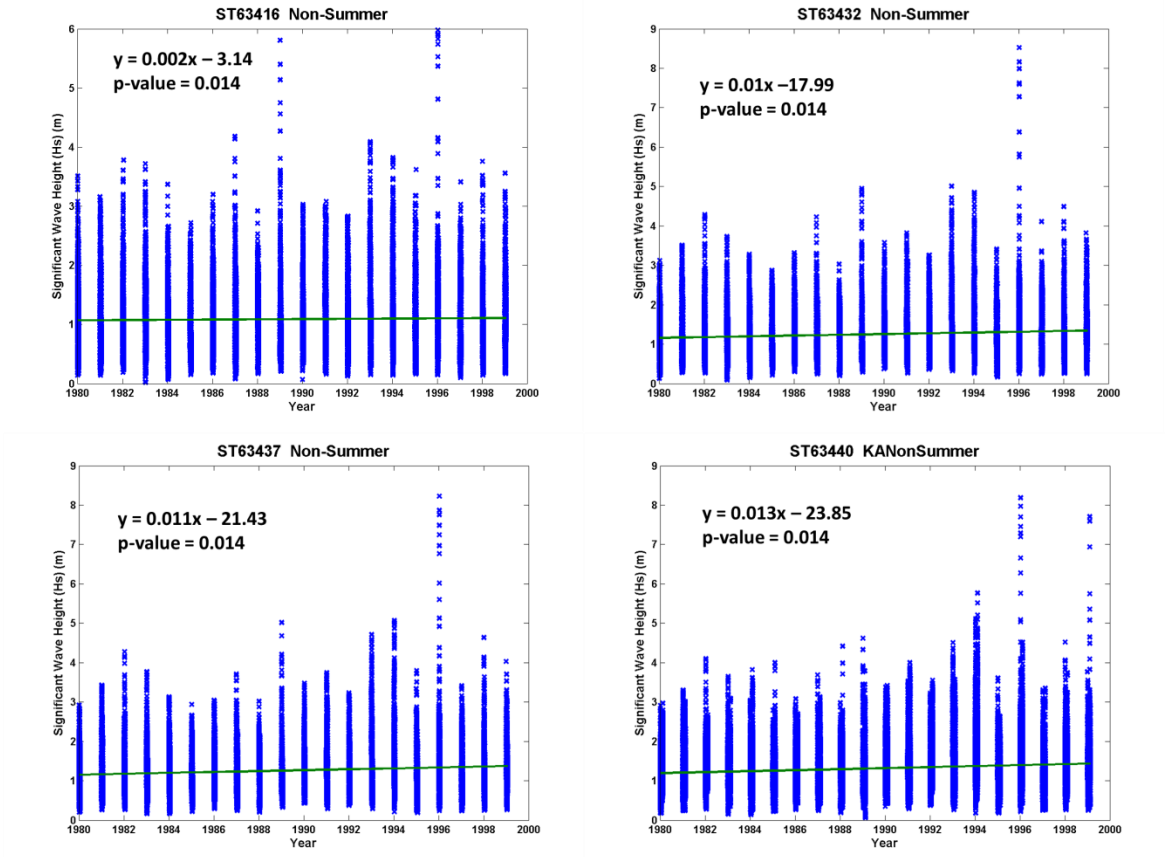

Figure 6. Significant wave height and trends for non-summer months for shallow WIS stations near Cape Canaveral, FL.

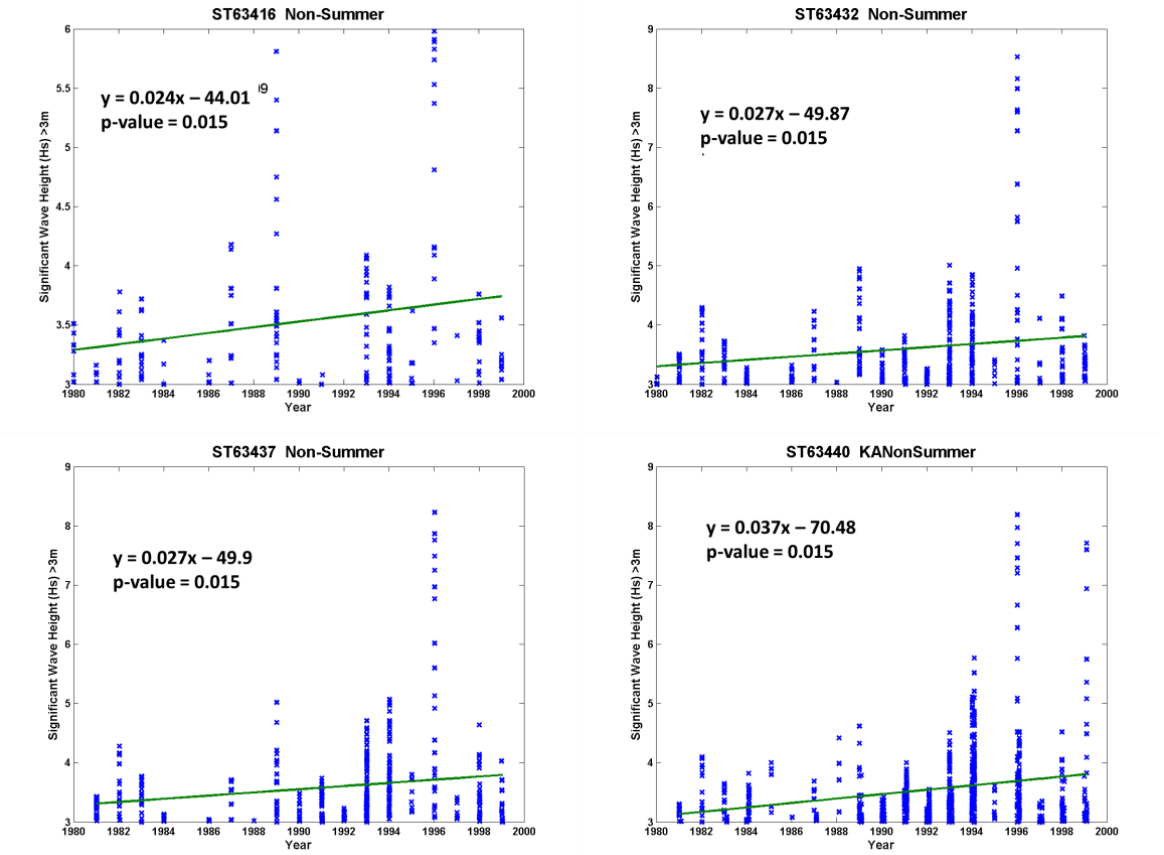

Figure 7. Wave heights greater than 3m and trends for nonsummer months from shallow water WIS stations near Cape Canaveral, FL.

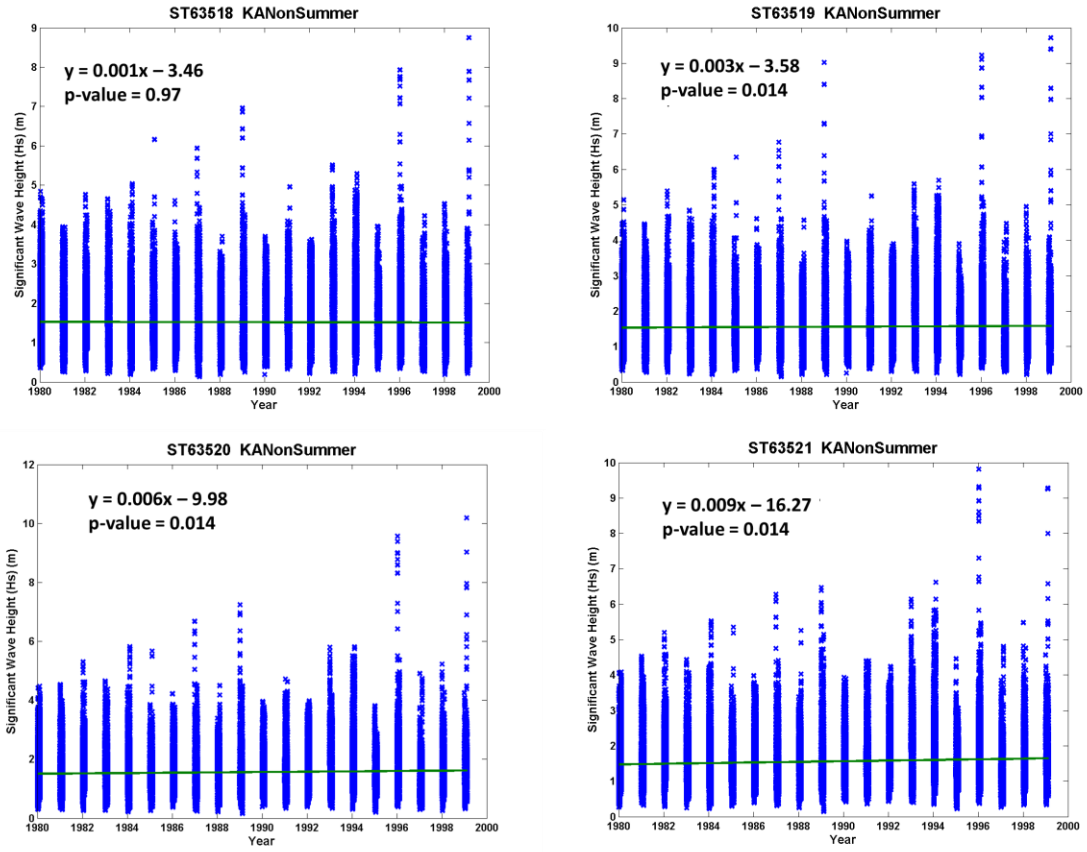

Figure 8. Significant wave height and trends for non-summer months from deep water WIS stations near Cape Canaveral, FL.

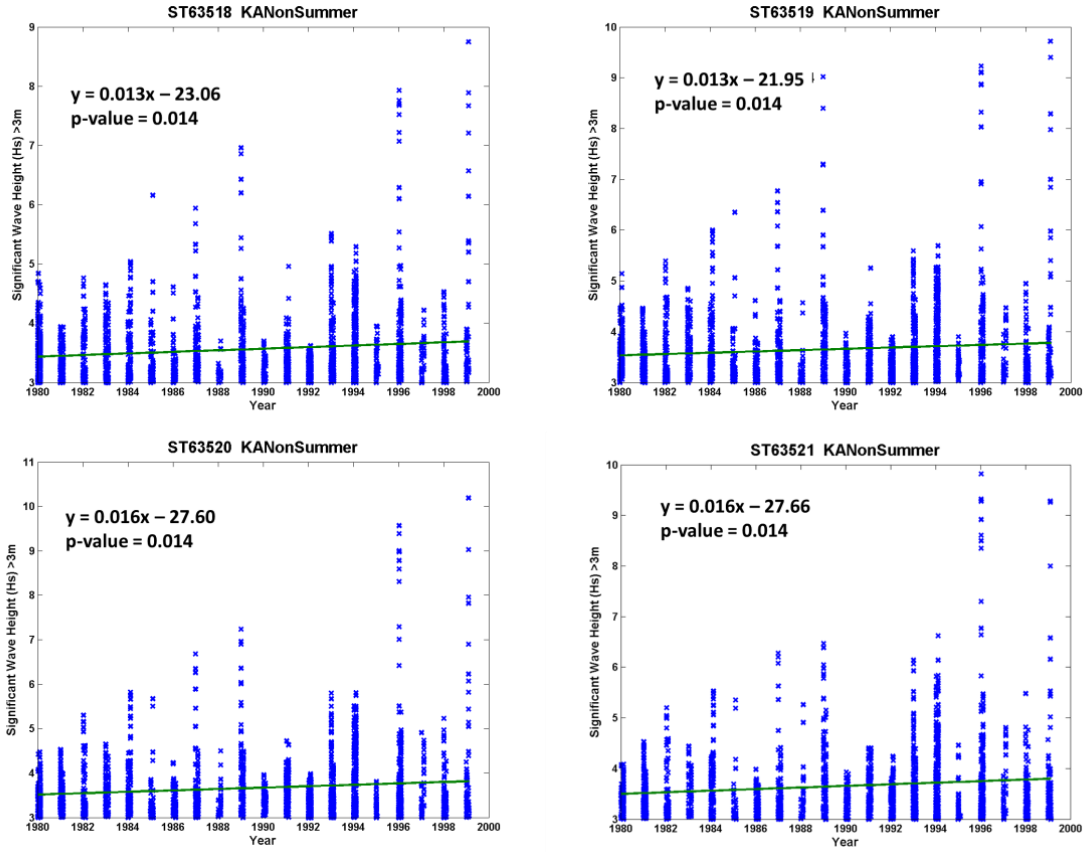

Figure 9. Significant wave height greater than 3m and trends for non-summer months from deep water WIS stations near Cape Canaveral, FL.

References

Absalonsen, L., and Dean, R. G. (2010), Characteristics of the Shoreline Change Along the Sandy Beaches of the State of Florida: An Atlas, No. FLSGP-M-10-001, pp. 1–304. National Sea Grant Library.

Adams P. N., D. L. Inman, and J. L. Lovering (2011), Effects of climate change and wave direction on longshore sediment transport patterns in Southern California, *Climatic Change*, **109**, 211-228. DOI: 10.1007/s10584-011-0317-0

Ashton, A., A. B. Murray, and O. Arnault (2001), Formation of coastline features by large-scale instabilities induced by high-angle waves, *Nature*, *414*, 296-300.

Ashton, A. D., and A. B. Murray (2006a), High-angle wave instability and emergent shoreline shapes: 1. Modeling of sand waves, flying spits, and capes, *Journal of Geophysical Research*, *111*(F04011).

Ashton, A. D., and A. B. Murray (2006b), High-angle wave instability and emergent shoreline shapes: 2. Wave climate analysis and comparisons to nature, *Journal of Geophysical Research: Earth Surface*, *111*(F4), 2156 - 2202.

Bromirski, P and J.P. Kossin (2008), Increasing hurricane wave power along the USAtlantic and Gulf coasts, *J. Geophys. Res.,113*, C07012, doi:10,1029/2007JC004706

Cleary, W.J. and Pilkey, O.H., Environmental Coastal Geology: Cape Lookout to Cape Fear, NC (Fieldtrip Guidebook). in Cleary, W.J., ed.,Environmental Coastal Geology: Cape Lookout to Cape Fear, NC. Carolina Geological Society Field Trip Guidebook 1996. p. 101-104.

Dolan, R., M.S. Fenster, S.J. Holme (1991) Temporal Analysis of Shoreline Recession and Accretion, *Journal of Coastal Research, 7* (3), 723 – 744.

Ells, K., and A. B. Murray (2012), Long-term, non-local coastline responses to local shoreline stabilization, *Geophys. Res. Lett.*, *39*(19), L19401.

Emanuel, K. (2005), Increasing destructiveness of tropical cyclones over the past 30 years, *Nature*, *436*, 686-688.

Ezer, T., L. P. Atkinson, W. B. Corlett, and J. L. Blanco (2013), Gulf Stream's induced sea level rise and variability along the U.S. mid-Atlantic coast, *Journal of Geophysical Research: Oceans*, *118*, 685-697.

Field, M. E., and D. B. Duane (1976), Post-Pleistocene history of the United States inner continental shelf: Significance to origin of barrier islands, *Geological Society of America Bulletin*, *87*, 691-702.

Finkl, C.W., J.E. Becerra, V. Achatz, J.L. Andrews (2008), Geomorphological Mapping along the Upper Southeast Florida Atlantic Continental Platform; I: Mapping Units, Symbolization and Geographic Information System Presentation of Interpreted Seafloor Topography, *Journal of Coastal Research, 24* (6) 1388 – 1417.

Florida Fish and Wildlife (FF&W), Florida Shoreline (1:12,000). Marine Resources Geographic System Internet Map Server. http://ocean.floridamarine.org/mrgis/Description_Layers_Marine.htm

Hayes, M.O. 1979. Barrier island morphology as a function of tidal and wave regime. In: Barrier Islands from the Gulf of St. Lawrence to the Gulf of Mexico, S.P. Leatherman (ed). New York: Academic Press. Pp. 1-27.

IPCC, Summary for Policymakers (SPM), *Climate Change 2007: The Physical Science Basis: Contribution of Working Group I to the Fourth Assessment Report of the Intergovernmental Panel on Climate Change*. Solomon, Ed. (Cambridge Univ. Press, New York, 2007).

Kemp, A. C., B. P. Horton, S. J. Culver, D. R. Corbett, O. van de Plassche, W. R. Gehrels, B. C. Douglas, and A. C. Parnell (2009), Timing and magnitude of recent accelerated sea-level rise (North Carolina, United States), *Geology*, *37*(11), 1035-1038, doi:10.1130/g30352a.1.

Knutson, T. R., J. L. McBride, J. Chan, K. Emanuel, G. Holland, C. Landsea, I. Held, J. P. Kossin, A. K. Srivastava, and M. Sugi (2010), Tropical cyclones and climate change, *Nature Geoscience*, *3*, 157 - 163.

Komar, P. D., and J. C. Allan (2008), Increasing Hurricane-Generated Wave Heights along the U.S. East Coast and Their Climate Controls, *Journal of Coastal Research*, *24*(2), 479-488, doi:10.2112/07-0894.1.

Leatherman, S. P., T. E. Rice, and V. Goldsmith (1982), Virginia Barrier Island Configuration: A Reappraisal, *Science*, *215*(4530), 285-287.

Lovejoy, D.W. (1983). The Anastasia Formation in Palm Beach and Martin counties, Florida. Miami Geological Society Memoir, 3, 58-72.

Magliocca, N. R., D. E. McNamara, and A. B. Murray (2011), Long-Term, Large-Scale Morphodynamic Effects of Artificial Dune Construction along a Barrier Island Coastline, *Journal of Coastal Research*, *27*(5), 918-930, doi:10.2112/jcoastres-d-10-00088.1.

McGranahan, G., D. Balk, and B. Anderson (April 2007), The rising tide: assessing the risks of climate change and human settlements in low elevation coastal zones, edited, pp. 17-37, Environment and Urbanization, doi:10.1177/0956247807076960.

McNamara, D., A. B. Murray, and M. D. Smith (2011), Coastal sustainability depends on how economic and coastline responses to climate change affect each other, *Geophysical Research Letters*, *38*, doi:10.1029/2011GL047207.

McNamara, D., and A. Keeler (2013), A coupled physical and economic model of the response of coastal real estate to climate risk, *Nature Climate Change*, **3**, pp. 559 – 562, doi:10.1038/nclimate1826

Moore, L. J. (2000), Shoreline mapping techniques, *Journal of Coastal Research*, *16*(1), 111-124.

Moore, L. J., J. H. List, S. J. Williams, and D. Stolper (2010), Complexities in barrier island response to sea level rise: Insights from numerical model experiments, North Carolina Outer Banks, *Journal of Geophysical Research-Earth Surface*, *115*, doi:F0300410.1029/2009jf001299.

Moore, L. J., D. E. McNamara, A. B. Murray, and O. Brenner (in review), Recent Shifts in Large-Scale Coastline Erosion Patterns Linked to Storm Climate Change, *Geophysical Research Letters*.

Moore, L. J., P. Ruggiero, and J. H. List (2006), Comparing mean high water and high, water line shorelines: Should proxy-datum offsets be incorporated into shoreline change analysis, *Journal of Coastal Research*, *22*(4), 894-905, doi:10.2112/104-0401.1.

National Aerounatics and Space Administration (NASA) (2010) Wallops Island VA Wallops Flight Center, Storm Damage Reduction Project Design for Wallops Island, Virginia (January 2010). Retrieved from http://sites.wff.nasa.gov/code250/docs/SRIPP_EIS_Appendix_A.pdf

National Oceanic and Atmospheric Administration (NOAA) (2012). National Geodetic Survey NOAA Shoreline Data Explorer, [URL:http://www.ngs.noaa.gov/newsys_ims/shoreline/index.cfm]

North Carolina Department of Earth and Environment – Division of Coastal Management. (2011). Oceanfront shorelines [Data file(s): 1998, 2003, 2004]

Retrieved from <http://dcm2.enr.state.nc.us/Maps/chdownload.htm#Oceanfront%20Shorelines

Oster, D. (2012) Beach Morphology of the Virginia Barrier Islands 1998, 2005, and 2009. Master's Thesis. University of Virginia. Accessed from

Pilkey, O. H., W. J. Neal, S. R. Riggs, C. A. Webb, D. M. Bush, D. F. Pilkey, J. Bullock, and B. A. Cowan (1998), *The North Carolina shore and its barrier islands, restless ribbons of sand*, Duke University Press, Durham.

Plant, N. G., and G. B. Griggs (1992), Interactions between Nearshore Processes and Beach Morphology Near a Seawall, *Journal of Coastal Research*, *8*(1), 183-200.

Program for the Study of Developed Shorelines (PSDS) (2012). Inventory of Coastal Engineering. [Data File(s): beachnourishment.zip] Retrieved from http://www.wcu.edu/9165.asp

Riggs, S. R., W. J. Cleary, and S. W. Snyder (1995), Influence of inherited geological framework on barrier shoreface morphology and dynamics, *Marine Geology*, *126*, 213-234.

Rink, W. J., and B. Forrest (2005), Dating Evidence for the Accretion History of Beach Ridges on Cape Canaveral and Merritt Island, Florida, USA, *Journal of Coastal Research*, *21*(5), 1000-1008.

Sallenger Jr., A. H., K. S. Doran, and P. A. Howd (2012), Hotspot of accelerated sea-level rise on the Atlantic coast of North America, *Nature Climate Change*, *2*, 884 - 888.

Slott, J. M., A. B. Murray, and A. D. Ashton (2010), Large-scale responses of complex-shaped coastlines to local shoreline stabilization and climate change, *Journal of Geophysical Research-Earth Surface*, *115*, doi:F0303310.1029/2009jf001486.

Slott, J. M., A. B. Murray, A. D. Ashton, and T. J. Crowley (2006), Coastline responses to changing storm patterns, *Geophysical Research Letters*, *33*(18), doi:L1840410.1029/2006gl027445.

Tait, J. F., and G. B. Griggs (1990), *Beach Response to the Presence of a Seawall*, 11-28 pp.

Thieler, E.R., Himmelstoss, E.A., Zichichi, J.L., and Ergul, Ayhan, Digital Shoreline Analysis System (DSAS) version 4.0—An ArcGIS extension for calculating shoreline change: U.S. Geological Survey Open-File Report 2008-1278.

USACE, 1965, Carolina Beach and Vicinity, Carolina Beach Portion (Coastal Storm Damage Reduction Program), Department of the Army, U.S. Corps of Engineers: Wilmington, NC

USACE, 1998, Carolina Beach and Vicinity, NC Area South, Kure Beach (Coastal Storm Damage Reduction Program), Department of the Army, U.S. Corps of Engineers: Wilmington, NC

United State Geological Survey (USGS) (2012). The National Assessment of Shoreline Change: A GIS Compilation of Vector Shorelines and Associated Shoreline Change Data for the New England and Mid-Atlantic Coasts. Open File Report 2010-1119[Data File(s): DelmarvaN_shorelines.shp, DelmarvaS_shorelines.shp] Retrieved from <http://pubs.usgs.gov/of/2010/1119/data_catalog.html>

United States Geological Survey (USGS) (2011). The National Assessment of Shoreline Change: A GIS Compilation of Vector Shorelines and Associated Shoreline Change Data for the U.S. Southeast Atlantic Coast. Open File Report 2005-1326. [Data file: nc_zip]. Retrieved from http://pubs.usgs.gov/of/2005/1326/gis-data.html

Valverde, H. R., A. C. Trembanis, and O. H. Pilkey (1999), Summary of beach nourishment episodes on the US East Coast barrier islands, *Journal of Coastal Research*, *15*(4), 1100-1118.

Wallops Island Flight Facility (WFF) (2011), NASA Seawall Extension at Wallops Island, VA, U.S Army Corps of Engineers Solicitation Number: W91236-11-B-0011, USACE District, Norfolk, Retreived from www.fbo.gov,

Wallops Island Flight Facility (WFF) (2010), Large ocean dredging and beach nourishment at significant distances (15 to 20 NM) from the Wallops Island coastline to be nourished and protected, U.S Army Corps of Engineers Solicitation Number: W91236-10-R-0026, USACE District, Norfolk, Retreived from www.fbo.gov,

Webster, P. J., G. J. Holland, J. A. Curry, and H.-R. Chang (2005), Changes in Tropical Cyclone Number, Duration, and Intensity in a Warming Environment, *Science*, *309*(5742), 1844-1846.

Werner, B. T., and D. E. McNamara (2007), Dynamics of coupled human-landscape systems, *Geomorphology*, *91*(3-4), 393-407, doi:10.1016/j.geomorph.2007.04.020.

Wolner, C.W.V, L.J. Moore, D.R. Young, S.T. Brantley, S.N. Bissett, R. A. McBride (2013), Ecomorphodynamic feedbacks and barrier island response to disturbance: Insights from the Virginia Barrier Islands, Mid-Atlantic Bight, USA. *Geomorphology*, doi: 10.1016/j.geomorph2013.03035, accepted manuscript

Work, P., and R. G. Dean (1990), *Shoreline Changes Adjacent to Florida's East Coast Tidal Inlets*, University of Florida, Coastal and Oceanographic Engineering Department.